

工學博士學位論文

$k-e-t$ 亂流 利用
流動 數值 研究

**A Numerical Study on In-Cylinder Flow Fields of an Engine
Using $k-e-t$ Turbulence Model**

指導教授 崔 在 星

2000 年 2 月

韓國海洋大學校 大學院

機關工學科 林 栽 文

Abstract.....	vi
Nomenclature.....	viii
1.	1
1.1	1
1.2	4
1.2.1	4
1.2.2	8
1.3	14
2.	17
2.1	17
2.1.1	17
2.1.2	18
2.1.3	20
2.2	23
2.3	28
2.3.1	29
2.3.2 $k - \mathbf{e}$	34
2.3.3 $k - \mathbf{e} - \mathbf{t}$	39
3.	44
3.1	44
3.2	50
3.2.1	50
3.2.2 SIMPLE	54

3.2.3 PISO	63
3.3	68
4.	70
4.1	70
4.1.1	70
4.1.2	72
4.2	73
4.3	75
4.4	80
4.5	84
4.6	100
4.7	115
5.	117
	120
1.	126
2.	130
3.	138

List of tables

Table 2.1	The diffusion coefficients and source terms of the conservation equations.....	22
Table 2.2	The source terms of the transformed conservation equations	27
Table 2.3	Values of coefficients appearing in the ϵ -equation according to different researcher.....	37
Table 2.4	The values of the model constants in the $k - \epsilon - t$ model.....	42
Table 4.1	Geometric details of model engine	71

List of figures

Fig.2.1	Coordinate system in cylinder	24
Fig.3.1	Grid structure and its notation	45
Fig.3.2	Control volume and its notation	46
Fig.3.3	u -control volume and its neighbouring velocity components.....	52
Fig.3.4	v -control volume and its neighbouring velocity components.....	53
Fig.3.5	The scalar control volume used for the discretization of the continuity equation.....	58
Fig.3.6	The SIMPLE algorithm.....	62
Fig.3.7	The PISO algorithm	67
Fig.4.1	Diagram of piston-cylinder assembly.....	71
Fig.4.2	Grid structure for numerical calculation.....	74
Fig.4.3	Radial profiles of axial mean velocity and rms velocity at $z=15\text{mm}$	
	(a) mean velocity at $\mathbf{q}=36^\circ$ (b) rms velocity at $\mathbf{q}=36^\circ$	77
	(c) mean velocity at $\mathbf{q}=90^\circ$ (d) rms velocity at $\mathbf{q}=90^\circ$	78
	(e) mean velocity at $\mathbf{q}=270^\circ$ (f) rms velocity at $\mathbf{q}=270^\circ$	79
Fig.4.4	Temporal changes of axial mean velocity at $z=15\text{mm}$, $r=25\text{mm}$	82
Fig.4.5	Temporal changes of turbulence intensity at $z=15\text{mm}$, $r=25\text{mm}$	83
Fig.4.6	Velocity fields of modified $k - \mathbf{e}$ model and $k - \mathbf{e} - \mathbf{t}$ model	
	(a) modified $k - \mathbf{e}$ model, $\mathbf{q}=36^\circ$ (b) $k - \mathbf{e} - \mathbf{t}$ model, $\mathbf{q}=36^\circ$	88
	(c) modified $k - \mathbf{e}$ model, $\mathbf{q}=90^\circ$ (d) $k - \mathbf{e} - \mathbf{t}$ model, $\mathbf{q}=90^\circ$	89
	(e) modified $k - \mathbf{e}$ model, $\mathbf{q}=180^\circ$ (f) $k - \mathbf{e} - \mathbf{t}$ model, $\mathbf{q}=180^\circ$...	90
	(g) modified $k - \mathbf{e}$ model, $\mathbf{q}=225^\circ$ (h) $k - \mathbf{e} - \mathbf{t}$ model, $\mathbf{q}=225^\circ$..	91
	(i) modified $k - \mathbf{e}$ model, $\mathbf{q}=270^\circ$ (j) $k - \mathbf{e} - \mathbf{t}$ model, $\mathbf{q}=270^\circ$...	92
	(k) modified $k - \mathbf{e}$ model, $\mathbf{q}=360^\circ$ (l) $k - \mathbf{e} - \mathbf{t}$ model, $\mathbf{q}=360^\circ$...	93
Fig.4.7	Turbulence intensities of modified $k - \mathbf{e}$ model and $k - \mathbf{e} - \mathbf{t}$ model	
	(a) modified $k - \mathbf{e}$ model, $\mathbf{q}=36^\circ$ (b) $k - \mathbf{e} - \mathbf{t}$ model, $\mathbf{q}=36^\circ$	94
	(c) modified $k - \mathbf{e}$ model, $\mathbf{q}=90^\circ$ (d) $k - \mathbf{e} - \mathbf{t}$ model, $\mathbf{q}=90^\circ$	95
	(e) modified $k - \mathbf{e}$ model, $\mathbf{q}=180^\circ$ (f) $k - \mathbf{e} - \mathbf{t}$ model, $\mathbf{q}=180^\circ$...	96

(g) modified $k - \epsilon$ model, $q=225^\circ$	(h) $k - \epsilon - t$ model, $q=225^\circ$	97	
(i) modified $k - \epsilon$ model, EMBED Equation.3	$q=270^\circ$ (j) EMBED Equation.3	model, EMBED Equation.3 $q=270^\circ$	
PAGEREF _Toc464642751 \h		98	
(k) modified EMBED Equation.3	$k - \epsilon$ $q=270^\circ$ $q=270^\circ$ $k - \epsilon$	99	
Fig.4.8	Diagram of piston-cylinder assembly with swirl vanes	101	
Fig.4.9	Radial profiles of axial mean velocity and rms velocity for SN=1.2 at $z=15\text{mm}, 40\text{mm}$		
(a) mean velocity at $q=90^\circ$	(b) rms velocity at $q=90^\circ$	104	
(c) mean velocity at $q=270^\circ$	(d) rms velocity at $q=270^\circ$	105	
Fig.4.10	Effects of swirl on axial velocity and rms velocity for SN=0.0, 1.2, 2.4 at $z=15\text{mm}$		
(a) mean velocity at $q=90^\circ$	(b) rms velocity at $q=90^\circ$	106	
(c) mean velocity at $q=270^\circ$	(d) rms velocity at $q=270^\circ$	107	
Fig.4.11	Effects of swirl on velocity fields at various crank angle s		
(a) SN=0.6, $q=36^\circ$	(b) SN=1.2, $q=36^\circ$	(c) SN=2.4, $q=36^\circ$	108
(d) SN=0.6, $q=90^\circ$	(e) SN=1.2, $q=90^\circ$	(f) SN=2.4, $q=90^\circ$	109
(g) SN=0.6, $q=270^\circ$	(h) SN=1.2, $q=270^\circ$	(i) SN=2.4, $q=270^\circ$	110
Fig.4.12	Effects of swirl on turbulence intensity fields at various crank angle s		
(a) SN=0.6, $q=36^\circ$	(b) SN=1.2, $q=36^\circ$	(c) SN=2.4, $q=36^\circ$	111
(d) SN=0.6, $q=90^\circ$	(e) SN=1.2, $q=90^\circ$	(f) SN=2.4, $q=90^\circ$	112
(g) SN=0.6, $q=270^\circ$	(h) SN=1.2, $q=270^\circ$	(i) SN=2.4, $q=270^\circ$	113
(j) SN=0.6, $q=360^\circ$	(k) SN=1.2, $q=360^\circ$	(l) SN=2.4, $q=360^\circ$	114
Fig.4.13	Velocity fields for different valve seat angle s at crank angle 36°		
(a) valve seat angle 30°	(b) valve seat angle 45°	(c) valve seat angle 60° ..	116

**A Numerical Study on In-Cylinder Flow Fields of an Engine
Using $k - \epsilon - \tau$ Turbulence Model**

Jae-Moon Lim

Department of Marine Engineering
Graduate School of Korea Maritime University

Abstract

This thesis describes and discusses the applicability of the $k - \epsilon - \tau$ turbulence model for calculation of the in-cylinder flow fields of an engine. The thesis also discusses the effects of swirl and valve seat angle to the characteristics of in-cylinder flow fields.

The equations are solved by finite difference method on a computational mesh which is made to always lie between the cylinder head and the moving piston head by defining a coordinate transformation which allows the axial grid line position to be expressed in terms of a time independent coordinate. The transformed conservation equations are integrated over the finite difference cells to provide algebraic equations. A hybrid differencing scheme is employed for numerical stability and PISO algorithm is used for the velocity-pressure coupling. $k - \epsilon - \tau$ turbulence model which considers the compressibility effect due to the compression and expansion of the

piston was used.

Calculations have been done for the intake and compression stroke cycle of a two dimensional axisymmetric model engine. The unsophisticated geometry has been selected for reasons of simplicity and saving computer time, so the main effort is focused on the treatment and understanding of the complex in-cylinder flow fields during intake and compression stroke cycle.

The predicted results using $k - \epsilon - \tau$ turbulence model of the turbulent flow fields in a model engine are compared to those from the modified $k - \epsilon$ turbulence model and the experimental data. The results obtained with the $k - \epsilon - \tau$ turbulence model are in much better agreement with the experimental data than the modified $k - \epsilon$ turbulence model, as far as the mean velocity and the turbulence intensity are concerned.

Finally the effects of swirl on the in-cylinder flow structure are examined through the parametric study of swirl numbers 0.0, 0.6, 1.2 and 2.4, then the effects of valve seat angle are examined. As the swirl number increases the center of the main vortex moves to the cylinder wall and the counterclockwise vortex increases near the intake valve. The turbulence intensity increases with swirl number during intake stroke, but it has a maximum value at swirl number 1.2 during compression stroke.

For the valve seat angle of 45° or more the flow pattern remains same but for the valve seat angle of 30° an alternative structure appears, in which the outer edge of the jet does not separate from the cylinder head wall, thus diminishing the corner vortex.

Nomenclature

a : Cell area

A : Total convective and diffusive flux coefficient

A_E : Effective flow area

A_R : Reference area

b_{ij} : Reynolds stress anisotropic tensor

$C_1, C'_1, C''_1, C_2, C_3, C_4, C_m$: Turbulence model constants

$C_5, C_{6,ISO}, C_{6,AXI}$: Turbulence model constants

C_D : Discharge coefficient

C_p : Specific heat at constant pressure

D : Velocity divergence

D_v : Valve head diameter

E : Empirical constant in the 'law of the wall'

f_1, f_2 : Spatial linear interpolation factors

h : Enthalpy

k : Turbulent energy

l : Turbulent length scale

L_v : Valve lift

\dot{m} : Mass flow rate

M : Mach number
 p : Pressure
 p^* : Gussed pressure
 p^{**} : Corrected pressure
 p^{***} : Twice corrected pressure
 p' : Pressure correction
 p'' : Second pressure correction
 P_{DIL} : Production of the turbulent energy by the dilatation part
 P_{INC} : Production of the turbulent energy by the incompressible part
 Pe : Peclet number
 P_{ij} : Production tensor
 P_T : Pressure at the throat
 q : Turbulent velocity
 q_w : Wall heat flux
 r : Radial coordinate direction
 R_{ij} : Reynolds stress tensor
 S_{AXI} : Mean strain rate for axisymmetric expansion flow
 S_{ISO} : Mean strain rate for isotropic compression flow
 s_{ij} : Strain rate tensor
 S_F : Source term for dependent variable f

T : Temperature
 $T_{ij}^{(1)}$: Rapid part of the pressure strain tensor
 T_w : Wall temperature
 u : Axial direction velocity
 \hat{u} : Relative velocity of the fluid
 u^*, v^* : Guessed velocities
 u^{**}, v^{**} : Corrected velocities
 u^{***}, v^{***} : Twice corrected velocities
 u', v' : Velocities corrections
 u^+ : Dimensionless velocity
 u_G : Grid velocity
 u_j : j-direction velocity
 u_t : Friction velocity
 v : Radial direction velocity
 w : Circumferential direction velocity
 x_j : j-coordinate direction
 y : Normal distance from the wall
 y^+ : Dimensionless distance
 z : Axial coordinate direction
 z_p : Instantaneous position of the piston

[Greek symbols]

\mathbf{a} : Spatial difference function in difference equation

\mathbf{a}_p : Pressure under-relaxation factor

$\mathbf{a}_u, \mathbf{a}_v$: Velocity under-relaxation factors

\mathbf{g} : Specific heat ratio

Γ_f : Diffusion coefficient

\mathbf{d}_{ij} : Kronecker delta

\mathbf{e} : Turbulent energy dissipation rate

\mathbf{q} : Circumferential coordinate direction

\mathbf{k} : Von Karman constant

\mathbf{m} : Viscosity

\mathbf{m}_{eff} : Effective viscosity

\mathbf{m} : Turbulent viscosity

\mathbf{n}_T : Turbulent kinematic viscosity

\mathbf{x} : Transformed axial coordinate

\mathbf{r} : Density

$\mathbf{s}_{T,l}$: Laminar Prandtl number

$\mathbf{s}_{T,t}$: Turbulent Prandtl number

\boldsymbol{t} : Turbulent time scale

\boldsymbol{f} : General dependent variable

Ω_{ij} : Mean rotation tensor

[Superscripts]

- : Ensemble mean value

' : Fluctuating component

n : New value

o : Old value

[Subscripts]

e, E : East

n, N : North

s, S : South

w, W : West

1.

1.1

1970 2

. 1980

가 ,

,

.

가

.

,

.

.

,

,

[1].

가

[2].

3

,

가

.

,

[3].

, LDA(laser doppler anemometer),

가

가

[4,5],

가

(non-stationary turbulent flow)

[6,7].

3

가

가

가

[8].

(zero dimensional)

,

(one

dimensional)

(multi dimensional)

[9].

가

가

. ,
, ,
, , , ,
.

,

가

가

[10]

,

,

,

.

,

가

,

,

,

.

.

,

.

1.2

1.2.1

(zero-dimensional) (one-dimensional)

[11]

1973 Watkins가

가

Watkins 2

1

가

Watkins^[11](1977) (ensemble

mean) , $k - e$

LDA

가

Watkins 가

4

1 Witze^[12]

가

Imperial College Gosman

Gosman and Johns^[13](1978)

가

(bowl)

TDC

aperture)

(annular

가

가

Ahmadi-Befrui et al.^[14](1982)

4

(vortex)

가

가

0.6

Gosman et al.^[15](1983)

3

, 가

,

. 가

annular

,

, 가

Grasso and Bracco^[16](1983)

2

TDC

$k - e$

2

Brandstatter et al.^[17](1985)

LDA

가

3

. 가

, 가

가

Yamada Toshio et al.^[18](1986)

가

3

가

가

가

. 가

가

. 가

Shah^[19](1989) $k - \epsilon$, $k - \epsilon$, $k - W$
 , Monaghan et al.^[20]
 $k - W$ 가

$k - \epsilon$ 3~10%
 $k - \epsilon$, $k - W$
 $k - W$

Mao et al.^[21](1994)
 ,
 FEM(finite element method) $k - \epsilon$
 (Watkins Morel)
 Lance et al.
 , FEM
 ,
 가

Khalighi^[22](1995) 가
 , 가
 , 가
 BDC (tumble) ,
 TDC

Kong et al.^[23](1997) KIVA-3

LDV

(squish)

1.2.2

3

(渦)

가

가

가

가

full field

modeling(FFM)

large eddy simulation(LES)

^[24]. FFM

(ensemble mean)

, 2

$k - \epsilon$

. LES

FFM

, LES FFM

subgrid scale model^[25]

. LES

$k - e$

가

$k - e$

k

e

$k - e$

-
-
-

가

가 ,

$k - e$

가

[26]

가

(time ratio)

,

가

$e -$

(production

term)

(dilatation)

$k - e$

$k - e$

, $e -$

가

Watkins^[11](1977), Reynolds^[27](1980), Morel and Mansour^[28](1982), El Tahry^[29](1983)가 $k - \mathbf{e}$.

Watkins(1977)

가

$k - \mathbf{e}$

^[11]. \mathbf{e} - \mathbf{reD} (D dilatation)

가 . Reynolds(1980) Watkins

(rapid spherical compression)

, (rapid

distortion theory)

\mathbf{e} -

(dilatation)

. Reynolds Gosman et al.^[30], Ramos et al.^[31], Grasso et al.^[32]

Morel and Mansour(1982)

, $k - \mathbf{e}$

가

$u_{i,i} < 0$

Reynolds

$S_e = c_3 \mathbf{re} u_{i,i}$, $c_3 < 0$

가 $c_3 > 0$

$k - \mathbf{e}$

$c_3 = 1$

Gosman et al.

$c_3 = 0$ Ramos et al.

Amadi-Befrui et al.^[33](1981) Reynolds

$c_3 = 1$

가

$c_3 = 0$

$c_3 = 0.373$

$c_3 = 0$

Ramos et al.

c_3

가

$c_3 > 0$

e-

가

$c_3 < 0$

El Tahry^[34](1982)

$k - e$

, OM(order of magnitude)

Gosman et al.

Watkins

가

$c_3 = -\frac{1}{3}$

$c_3 = 0.373$

El Tahry^[35](1984) $k - \epsilon$

가

가

Launder et al.^[36]

Reynolds

.

,

7

(6 ϵ)

가

Wu et al.^[37](1985)

1

, Navier-Stokes

$k - \epsilon$

가

$k - \epsilon$

,

. $k - \epsilon$

가

,

가

가

Wu et al.

' t '

$k - \epsilon - t$

$k - \epsilon - t$

,

,

,

Shah and Markatos^[38](1987) 2, 3 Ilgbusi

Spalding^[39]

$k - W$

$k - W$

$k - \mathbf{e}$

, $k - W$

$k - \mathbf{e}$

Naser et al.^[40](1995)

/

/

, 가

$k - \mathbf{e}$

,

1

two-layer

two-layer

$k - \mathbf{e}$

$k - \mathbf{e}$

, two-layer

/

Watkins et al.^[41](1996) DSM(differential stress model)

, DSM

, $k - \mathbf{e}$

DSM

가 $k - \mathbf{e}$

DSM

가 $k - \mathbf{e}$

TDC

DSM

가

RNG(renormalization group) $k - \mathbf{e}$

가

[42,43,44]

가 ,

, Wu et al.가

$k - \mathbf{e} - \mathbf{t}$

1.3

가

$k - \mathbf{e} - \mathbf{t}$

2, 3, 4, 5

2

[45,46]

가

(ensemble averaged)

$k - e$

가

$k - e$

$k - e - t$

3

가

Peclet

Peclet

가

(staggered grid)

1

(predictor step)

2

(corrector step)

가

가

PISO

4

$k - e - t$

Ahmadi-Befrui^[14]

$k - e$

$k - e - t$

가

$k - e - t$

Arcoumanis^[47]

0.6,

1.2, 2.4

60 ° , 45 ° , 30 °

5

$k - e - t$

2.

2.1

가 . 2.1.2
(ensemble averaged
form)
(phase)
가 . (closing)
가
[11].

2.1.1

(stagnation enthalpy) , 가
[19],

$$\frac{\partial \mathbf{r}}{\partial t} + \frac{\partial}{\partial x_j} (\mathbf{r} u_j) = 0 \quad (2.1)$$

$$\frac{\partial}{\partial t} (\mathbf{r} u_i) + \frac{\partial}{\partial x_j} (\mathbf{r} u_j u_i) = -\frac{\partial p}{\partial x_i} + \frac{\partial}{\partial x_j} \left(\mathbf{m} \frac{\partial u_i}{\partial x_j} \right) + S_{u_i} \quad (2.2)$$

$$\frac{\partial}{\partial t} (\mathbf{r} h) + \frac{\partial}{\partial x_j} (\mathbf{r} u_j h) = \frac{\partial p}{\partial t} + \frac{\partial}{\partial x_j} \left[\Gamma_h \frac{\partial h}{\partial x_j} \right] + S_h \quad (2.3)$$

$$\mathbf{m}, \Gamma_h, S_{u_i}, S_h$$

(body force),

$$\frac{\partial}{\partial t} (\mathbf{r} \mathbf{f}) + \frac{\partial}{\partial x_i} (\mathbf{r} u_i \mathbf{f}) = \frac{\partial}{\partial x_i} \left[\Gamma_f \frac{\partial \mathbf{f}}{\partial x_i} \right] + S_f \quad (2.4)$$

(a) (b) (c) (d)

$$\mathbf{f}, \Gamma_f, S_f$$

(2.4) (a) \mathbf{f} (local rate of change), (b) (c)

3, \mathbf{f}

(d) \mathbf{f}

2.1.2

1)

,

.

,

.

(

)

$$f(\mathbf{q}, i) = \bar{f}(\mathbf{q}) + f'(\mathbf{q}, i) \quad (2.5)$$

$$\bar{f}(\mathbf{q}) = \lim_{N \rightarrow \infty} \frac{1}{N} \sum_{i=1}^N f(\mathbf{q}, i) \quad (2.6)$$

$$f'(\mathbf{q}, i) = \lim_{N \rightarrow \infty} \frac{1}{N} \left[\sum_{i=1}^N (f(\mathbf{q}, i) - \bar{f}(\mathbf{q}))^2 \right]^{\frac{1}{2}} \quad (2.7)$$

2)

,

.

(2.5)

(2.6)

(2.4)

$$\frac{\partial}{\partial t}(\mathbf{r}\bar{\mathbf{f}}) + \frac{\partial}{\partial x_i}(\mathbf{r}\bar{u}_i\bar{\mathbf{f}}) = \frac{\partial}{\partial x_i} \left[\Gamma_{\bar{\mathbf{f}}} \frac{\partial \bar{\mathbf{f}}}{\partial x_i} \right] + \bar{S}_{\bar{\mathbf{f}}} + \frac{\partial}{\partial x_i} \overline{\mathbf{r}u'_i\mathbf{f}} \quad (2.8)$$

(2.8) (2.4)

$$(2.8) \quad \bar{\mathbf{f}}$$

가 $\bar{\mathbf{f}}$ u_j 가

$$\overline{\mathbf{r}u'_i\mathbf{f}} = -\overline{\mathbf{r}u'_i u'_j} \quad (2.9)$$

$-\overline{\mathbf{r}u'_i u'_j}$, 가

$\overline{u'_i u'_j}$ (fluctuation velocity)

, $\overline{u'_i\mathbf{f}}$ -

(eddy viscosity concept) . 2.3.1

2.1.3

(2.10) [19].

$$\begin{aligned} & \frac{\partial}{\partial t}(\mathbf{r}\mathbf{f}) + \frac{\partial}{\partial z}(\mathbf{u}\mathbf{f}) + \frac{1}{r} \frac{\partial}{\partial r}(r\mathbf{r}\mathbf{v}\mathbf{f}) + \frac{1}{r} \frac{\partial}{\partial \mathbf{q}}(\mathbf{r}\mathbf{w}\mathbf{f}) \\ &= \frac{\partial}{\partial z} \left[\Gamma_f \frac{\partial \mathbf{f}}{\partial z} \right] + \frac{1}{r} \frac{\partial}{\partial r} \left[r\Gamma_f \frac{\partial \mathbf{f}}{\partial r} \right] + \frac{1}{r^2} \frac{\partial}{\partial \mathbf{q}} \left[\frac{\Gamma_f}{r} \frac{\partial \mathbf{f}}{\partial \mathbf{q}} \right] + S_f \end{aligned} \quad (2.10)$$

u, v, w , , , \mathbf{f} , \mathbf{r} , Γ_f , S_f .

(2.10) $\mathbf{f}=1$.

$$\frac{\partial \mathbf{r}}{\partial t} + \frac{\partial}{\partial z}(\mathbf{r}\mathbf{u}) + \frac{1}{r} \frac{\partial}{\partial r}(r\mathbf{r}\mathbf{v}) + \frac{1}{r} \frac{\partial}{\partial \mathbf{q}}(\mathbf{r}\mathbf{w}) = 0 \quad (2.11)$$

가 $\frac{\partial}{\partial \mathbf{q}} = 0$,

$$\frac{\partial \mathbf{r}}{\partial t} + \frac{\partial}{\partial z}(\mathbf{r}\mathbf{u}) + \frac{1}{r} \frac{\partial}{\partial r}(r\mathbf{r}\mathbf{v}) = 0 \quad (2.12)$$

$$\begin{aligned} & \frac{\partial}{\partial t}(\mathbf{r}\mathbf{f}) + \frac{\partial}{\partial z}(\mathbf{u}\mathbf{f}) + \frac{1}{r} \frac{\partial}{\partial r}(r\mathbf{r}\mathbf{v}\mathbf{f}) \\ &= \frac{\partial}{\partial z} \left[\Gamma_f \frac{\partial \mathbf{f}}{\partial z} \right] + \frac{1}{r} \frac{\partial}{\partial r} \left[r\Gamma_f \frac{\partial \mathbf{f}}{\partial r} \right] + S_{f(z,r)} \end{aligned} \quad (2.13)$$

Γ_f S_f Table 2.1 .

Table 2.1 The diffusion coefficients and source terms of the conservation equations

f	Γ_f	$(S_f)_{z,r}$
1	0	0
u	\mathbf{m}_{eff}	$-\frac{\partial p}{\partial z} + \frac{\partial}{\partial z} \left(\mathbf{m}_{eff} \frac{\partial u}{\partial z} \right) + \frac{1}{r} \frac{\partial}{\partial r} \left(r \mathbf{m}_{eff} \frac{\partial v}{\partial z} \right)$ $-\frac{2}{3} \frac{\partial}{\partial z} \left(\mathbf{m}_{eff} \nabla \cdot \underline{u} + r k \right)$
v	\mathbf{m}_{eff}	$-\frac{\partial p}{\partial r} + \frac{\partial}{\partial z} \left(\mathbf{m}_{eff} \frac{\partial u}{\partial r} \right) + \frac{1}{r} \frac{\partial}{\partial r} \left(r \mathbf{m}_{eff} \frac{\partial v}{\partial r} \right)$ $+ r \frac{w^2}{r} - 2 \mathbf{m}_{eff} \frac{v}{r^2} - \frac{2}{3} \frac{\partial}{\partial r} \left(\mathbf{m}_{eff} \nabla \cdot \underline{u} + r k \right)$
w	\mathbf{m}_{eff}	$-\frac{\partial r}{\partial q} - \frac{2}{r} \frac{\partial}{\partial r} \left(r \mathbf{m}_{eff} w \right) - 2 \mathbf{m}_{eff} \frac{v}{r^2} + \frac{r w^2}{r^3}$
h	$\frac{\mathbf{m}_{eff}}{\mathbf{S}_h}$	$\frac{\partial p}{\partial t}$
		$\nabla \cdot \underline{u} = \frac{\partial u}{\partial z} + \frac{1}{r} \frac{\partial}{\partial r} (rv)$

2.2

, Eulerian

Eulerian-Lagrangian

()

(z, r, t) (\mathbf{x}, r, t)

\mathbf{x}

[48]

$$\mathbf{x} = \frac{z}{z_p} \quad (2.14)$$

z_p t , Fig.2.1

(2.14)

z t

$$\frac{\partial \mathbf{x}}{\partial z} = \frac{1}{z_p}$$

$$\frac{\partial \mathbf{x}}{\partial t} = -\frac{z}{z_p^2} \frac{dz_p}{dt} = -\frac{\mathbf{x}}{z_p} \frac{dz_p}{dt} \quad (2.15)$$

\mathbf{f} \mathbf{f}

\mathbf{f}

가

$$\mathbf{f}(z, r, t) \equiv \mathbf{f}(\mathbf{x}, r, t) \quad (2.16)$$

\mathbf{f}

$$d\mathbf{f} = \frac{\partial \mathbf{f}}{\partial z} dz + \frac{\partial \mathbf{f}}{\partial r} dr + \frac{\partial \mathbf{f}}{\partial t} dt \quad (2.17)$$

$$d\mathbf{f} = \frac{\partial \mathbf{f}}{\partial \mathbf{x}} d\mathbf{x} + \frac{\partial \mathbf{f}}{\partial r} dr + \frac{\partial \mathbf{f}}{\partial t} dt \quad (2.18)$$

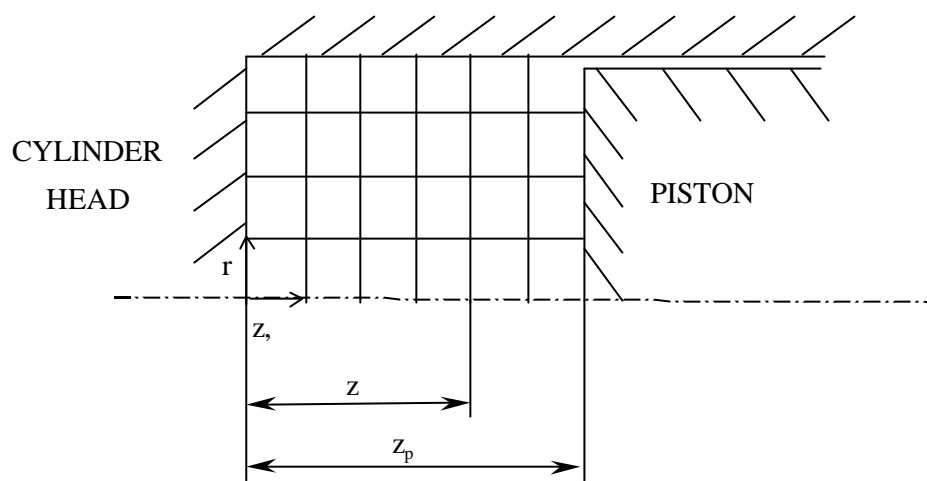


Fig.2.1 Coordinate system in cylinder

$$d\mathbf{x} = \frac{\partial \mathbf{x}}{\partial z} dz + \frac{\partial \mathbf{x}}{\partial t} dt \quad (2.19)$$

(2.19) (2.18)

$$d\mathbf{f} = \frac{\partial \mathbf{f}}{\partial \mathbf{x}} \frac{\partial \mathbf{x}}{\partial z} dz + \frac{\partial \mathbf{f}}{\partial \mathbf{x}} \frac{\partial \mathbf{x}}{\partial t} dt + \frac{\partial \mathbf{f}}{\partial r} dr + \frac{\partial \mathbf{f}}{\partial t} dt \quad (2.20)$$

(2.17) (2.20)

$$\begin{aligned} \frac{\partial \mathbf{f}}{\partial z} &= \frac{\partial \mathbf{f}}{\partial \mathbf{x}} \frac{\partial \mathbf{x}}{\partial z} \\ \frac{\partial \mathbf{f}}{\partial r} &= \frac{\partial \mathbf{f}}{\partial r} \\ \frac{\partial \mathbf{f}}{\partial t} &= \frac{\partial \mathbf{f}}{\partial \mathbf{x}} \frac{\partial \mathbf{x}}{\partial t} + \frac{\partial \mathbf{f}}{\partial t} \end{aligned} \quad (2.21)$$

(2.15) (2.21)

$$\begin{aligned} \frac{\partial \mathbf{f}}{\partial z} &= \frac{1}{z_p} \frac{\partial \mathbf{f}}{\partial \mathbf{x}} \\ \frac{\partial \mathbf{f}}{\partial r} &= \frac{\partial \mathbf{f}}{\partial r} \\ \frac{\partial \mathbf{f}}{\partial t} &= \frac{\partial \mathbf{f}}{\partial t} - \frac{\mathbf{x}}{z_p} \frac{dz_p}{dt} \frac{\partial \mathbf{f}}{\partial \mathbf{x}} \end{aligned} \quad (2.22)$$

(2.22) (2.13)

$$\begin{aligned} &\frac{\partial}{\partial t}(\mathbf{r}\mathbf{f}) - \frac{\mathbf{x}}{z_p} \frac{dz_p}{dt} \frac{\partial}{\partial \mathbf{x}}(\mathbf{r}\mathbf{f}) + \frac{1}{z_p} \frac{\partial}{\partial \mathbf{x}}(\mathbf{r}\mathbf{f}) + \frac{1}{r} \frac{\partial}{\partial r}(\mathbf{r}\mathbf{f}) \\ &= \frac{1}{z_p} \frac{\partial}{\partial \mathbf{x}} \left[\frac{\Gamma_f}{z_p} \frac{\partial \mathbf{f}}{\partial \mathbf{x}} \right] + \frac{1}{r} \left[\frac{\partial}{\partial r} r \Gamma_f \frac{\partial \mathbf{f}}{\partial r} \right] + S_f \end{aligned} \quad (2.23)$$

$$\frac{1}{z_p} \frac{\partial}{\partial t} (\mathbf{r} \mathbf{f}_{z_p}) = \frac{1}{z_p} \frac{dz_p}{dt} \mathbf{r} \mathbf{f} + \frac{\partial}{\partial t} (\mathbf{r} \mathbf{f})$$

$$\frac{1}{z_p} \frac{\partial}{\partial \mathbf{x}} (\mathbf{r} \hat{u} \mathbf{f}) = \frac{1}{z_p} \frac{\partial}{\partial \mathbf{x}} \left[\mathbf{r} \left(\hat{u} - \mathbf{x} \frac{dz_p}{dt} \right) \mathbf{f} \right] \quad (2.24)$$

$$, (2.24) \quad (2.23)$$

$$\begin{aligned} & \frac{1}{z_p} \frac{\partial}{\partial t} (\mathbf{r} z_p \mathbf{f}') + \frac{1}{z_p} \frac{\partial}{\partial \mathbf{x}} (\mathbf{r} \hat{u} \mathbf{f}') + \frac{1}{r} \frac{\partial}{\partial r} (r \mathbf{r} v \mathbf{f}') \\ & = \frac{1}{z_p} \frac{\partial}{\partial \mathbf{x}} \left(\frac{\Gamma_f}{z_p} \frac{\partial \mathbf{f}'}{\partial \mathbf{x}} \right) + \frac{1}{r} \frac{\partial}{\partial r} \left(r \Gamma_f \frac{\partial \mathbf{f}'}{\partial r} \right) + (S_f)_{x,r} \end{aligned} \quad (2.25)$$

$$\hat{u} = u - u_G \quad (2.26)$$

$$u_G \equiv \mathbf{x} \frac{dz_p}{dt} \quad (2.27)$$

$(S_f)_{x,r}$ Table 2.2

Table 2.2 The source terms of the transformed conservation equations

f'	$(S_f)_{x,r}$
\hat{u}	$-\frac{1}{z_p} \frac{\partial \mathbf{r}}{\partial \mathbf{x}} + \frac{1}{z_p} \frac{\partial}{\partial \mathbf{x}} \left(\frac{\mathbf{m}_{eff}}{z_p} \frac{\partial u}{\partial \mathbf{x}} \right) + \frac{1}{r} \frac{\partial}{\partial r} \left(\frac{r \mathbf{m}_{eff}}{z_p} \frac{\partial v}{\partial \mathbf{x}} \right)$ $-\frac{2}{3} \frac{1}{z_p} \frac{\partial}{\partial \mathbf{x}} (\mathbf{m}_{eff} \nabla \cdot \underline{u} + \mathbf{r}k) - \frac{1}{z_p} (\mathbf{r} z_p u_G)$ $-\frac{1}{z_p} \frac{\partial}{\partial \mathbf{x}} \left(\mathbf{r} u u_G - \frac{1}{z_p} \frac{\partial u_G}{\partial \mathbf{x}} \right) - \frac{1}{r} \frac{\partial}{\partial r} \left(\mathbf{r} \mathbf{r} v u_G - r \mathbf{m}_{eff} \frac{\partial u_G}{\partial r} \right)$
v	$-\frac{\partial p}{\partial r} + \frac{1}{z_p} \frac{\partial}{\partial \mathbf{x}} \left(\mathbf{m}_{eff} \frac{\partial u}{\partial r} \right) + \frac{1}{r} \frac{\partial}{\partial r} \left(r \mathbf{m}_{eff} \frac{\partial v}{\partial r} \right) + \mathbf{r} \frac{w^2}{r} - 2 \mathbf{m}_{eff} \frac{v}{r^2}$ $-\frac{2}{3} \frac{\partial}{\partial r} (\mathbf{m}_{eff} \nabla \cdot \underline{u} + \mathbf{r}k)$
w	$-\frac{\partial \mathbf{r}}{\partial \mathbf{q}} - \frac{2}{r} \frac{\partial}{\partial r} (r \mathbf{m}_{eff} w) - 2 \mathbf{m}_{eff} \frac{v}{r^2} + \frac{\mathbf{r} w^2}{r^3}$
h	$\frac{\partial p}{\partial t} - \frac{\mathbf{x}}{z_p} \frac{dz_p}{dt} \frac{\partial p}{\partial \mathbf{x}}$
	$\nabla \cdot u = \frac{1}{z_p} \frac{\partial u}{\partial \mathbf{x}} + \frac{1}{r} \frac{\partial}{\partial r} (r v)$

2.3

가

가

$t = m \frac{\eta u}{\eta y}$ 가 , Navier-

Stokes

(scale) 가

가

m m

(Reynolds) , t_T

t_T

[49]

2.3.1

가

.

.

,

,

.

가

.

가 가 ,

가 .

.

full-field modeling(FFM)

[49].

Boussinesq

(eddy diffusivity)

.

m

, 1

, 2

.

FFM

,

large eddy simulation(LES)

subgrid scale model^[25]

.

.

1) ()

,

(zero)

Prandtl (mixing length)

.

(mean free path)

,

가

,

, 3

.

2) 1

n_T

,

\sqrt{k}

,

l

n_T

C

.

$$n_T = C\sqrt{kl}$$

(2.28)

Prandtl-Kolmogorov

. k

, l

1

, k

l

2

.

, 1

,

,

,

,

, (length scale)

1

가

() 가

3) 2

2 1

Navier-Stokes l

Navier-Stokes

가 \mathbf{e} , $k - \mathbf{e}$

2 가

○ k \mathbf{e}

○ Navier-Stokes \mathbf{e}

○ near-wall correction

4) $k - \mathbf{e}$

$$\begin{aligned}
 & k \\
 & \mathbf{e} \\
 & l \\
 & \mathbf{e} \\
 & \mathbf{e} = \frac{k^{\frac{3}{2}}}{l} \quad (2.29)
 \end{aligned}$$

$$\begin{aligned}
 & \mathbf{n}_T \quad C_m \\
 & \mathbf{n}_T = \frac{C_m k^2}{\mathbf{e}} \quad (2.30)
 \end{aligned}$$

$k \mathbf{e}$ \mathbf{n}_T 가 2

$$\begin{aligned}
 & k \\
 & u \frac{\mathcal{I}k}{\mathcal{I}x} + v \frac{\mathcal{I}k}{\mathcal{I}y} = \mathbf{n}_T \left(\frac{\mathcal{I}u}{\mathcal{I}y} \right)^2 - \mathbf{e} + \frac{\mathcal{I}}{\mathcal{I}y} \left(\frac{\mathbf{n}_T \mathcal{I}k}{\mathcal{S}_k \mathcal{I}y} \right) \quad (2.31)
 \end{aligned}$$

\mathbf{e} 3

$$u \frac{\overline{\rho e}}{\overline{\rho k}} + \nu \frac{\overline{\rho e}}{\overline{\rho \nu}} = C_1 \frac{\overline{\rho \epsilon}}{k} \left(\frac{\overline{\rho \mu}}{\overline{\rho \nu}} \right)^2 - C_2 \frac{\overline{\rho \epsilon}^2}{k} + \frac{\overline{\rho \nu}}{\overline{\rho \nu}} \left(\frac{\overline{\rho \epsilon}}{\overline{\rho \nu}} \right) \quad (2.32)$$

5

[26]

$$C_m = 0.09, \quad C_1 = 1.45, \quad C_2 = 1.9, \quad \mathbf{s}_k = 1.0, \quad \mathbf{s}_\epsilon = 1.3 \quad (2.33)$$

Spalding-Launder $k - \epsilon$

$k - \epsilon$

[50],

Watkins^[11])

$k - \epsilon$

(Reynolds^[27])

Morel and Mansour^[28], El Thary^[29]

$k - \epsilon$

$k - \epsilon$

2.3.2

5)

가

[51,52]

3

7 (

6 ,

1) 가

,

6) LES

LES

, Navier-Stokes

.

subgrid scale model

. LES

, 가

가 .

,

가

,

.

2.3.2 $k - \epsilon$

가 .

,

,

$k - \epsilon$

$k - \epsilon$

1

가

[53].

$k - e$

가

[26].

가

(time ratio)

.

.

$k - e$

[127].

Watkins^[11]

가

$k - e$

, $re\vec{v} \cdot u$

(dilatation)

$e-$

가

Watkins

. Renyolds^[27] Watkins

(rapid spherical

compression)

,

(dilatation)

.

, Morel and Mansour^[28], El Thary^[29]

$$k - \mathbf{e} \quad k$$

$$\begin{aligned} \frac{\partial}{\partial t}(\mathbf{rk}) + \frac{\partial}{\partial x_j}(\mathbf{rk}u_j) &= \frac{\partial}{\partial x_j} \left(\frac{\mathbf{m}}{\mathbf{s}_k} \frac{\partial k}{\partial x_j} \right) \\ &+ 2\mathbf{m} s_{ij} s_{ij} - \frac{2}{3}(\mathbf{m}D^2 + \mathbf{rk}D) - \mathbf{re} \end{aligned} \quad (2.34)$$

\mathbf{e} -

$$\begin{aligned} \frac{\partial}{\partial t}(\mathbf{re}) + \frac{\partial}{\partial x_j}(\mathbf{re}u_j) &= \frac{\partial}{\partial x_j} \left(\frac{\mathbf{m}}{\mathbf{s}_e} \frac{\partial \mathbf{e}}{\partial x_j} \right) \\ &+ \frac{\mathbf{e}}{k} \left[2C_1 \mathbf{m} s_{ij} s_{ij} - \frac{2}{3}(C'_1 \mathbf{m}D^2 + C''_1 \mathbf{rk}D) \right] \\ &+ C_3 \mathbf{re}D + C_4 \frac{\mathbf{re}}{\mathbf{m}} \frac{\partial \mathbf{m}}{\partial t} - C_2 \frac{\mathbf{re}^2}{k} \end{aligned} \quad (2.35)$$

\mathbf{r} , \mathbf{s} , u_j x_j j -

, s_{ij}

$$s_{ij} = \frac{1}{2} \left(\frac{\partial u_i}{\partial x_j} + \frac{\partial u_j}{\partial x_i} \right) \quad (2.36)$$

D divergence

$$D = s_{ii} \equiv \nabla \cdot \mathbf{u} \quad (2.37)$$

m

$$m = \frac{C_m r k^2}{e} \quad (2.38)$$

C_m

C_1', C_1'' Table 2.3

Table 2.3 Values of coefficients appearing in the e -equation according to different researcher

researchers	C_1	C_1'	C_1''	C_2	C_3	C_4
Watkins	1.44	1.44	1.44	1.92	1	0
Reynolds	1.44	1.44	1.44	1.92	-0.373	0
Morel and Mansour	1.44	1.32~1.44	3.5~4.5	1.92	1	0
El Tahry	1.44	1.44	1.44	1.92	-1/3	1

Watkins

Reynolds

$$C_3 = \frac{2}{3}(2 - C_1) \quad (2.39)$$

$$C_3 = -\frac{2}{3}(2 - C_1)$$

Morel and Mansour 가

Reynolds

, C_1' C_1'' 가 가 . Table 2.3

El Tahry . $C_3 = -\frac{1}{3}$

, 가 .

$$C_4 \frac{\mathbf{re} \partial \mathbf{m}}{\mathbf{m} \partial t} \quad (2.40)$$

\mathbf{m} . \mathbf{m} ,

/ 가 .

$$C_4 \mathbf{re} \nabla \cdot \mathbf{u} \quad (2.41)$$

C_3 C_4

, ()

\mathbf{e} - 가 .

○ $\mathbf{t} = \begin{pmatrix} k \\ \mathbf{e} \end{pmatrix}$

, 가 \mathbf{t} .

○ \mathbf{e} k $C_3 - \frac{2}{3} C_1''$

. $C_3 < \frac{2}{3} C_1''$

○ , $C_4 > 0$ 가

Table 2.3

Watkins

e

e

가

Wu et al.^[37]

Watkins

Reynolds

1

k

l

Navier-Stokes

가

e-

t

가

s⁻¹

가

k-e-t

2.3.3 **k-e-t**

1

가 가

가

가

가, 가, Kolmogorov

가, 가

가

Wu et al.^[37](1985) 1

, Navier-Stokes

$k - \epsilon$ 가 .

$k - \epsilon$,

가

Kolmogorov . $k - \epsilon$

가 ,

가

가 Wu et al.

' t ' ,

$k - \epsilon - t$.

$k - \epsilon - t$

$$k - \mathbf{e}$$

$$k - \mathbf{e} - \mathbf{t}$$

[37]

$$\frac{dk}{dt} = P_{INC} + P_{DIL} - \mathbf{e} \quad (2.42)$$

$$\frac{d\mathbf{e}}{dt} = -\frac{\mathbf{e}}{\mathbf{t}} + C_1 \frac{P_{INC} \mathbf{e}}{k} + C_4 \frac{P_{DIL} \mathbf{e}}{k} \quad (2.43)$$

$$\frac{d\mathbf{t}}{dt} = \frac{5}{11} + C_5 \left(\frac{\mathbf{e}\mathbf{t}}{k} - \frac{6}{11} \right) + C_{6,ISO} S_{ISO} \mathbf{t} + C_{6,AXI} S_{AXI} \mathbf{t} \quad (2.44)$$

$$P_{INC} = -R_{ij} \left(\bar{u}_{i,j} - \frac{1}{3} \bar{u}_{k,k} \mathbf{d}_{ij} \right)$$

$$P_{DIL} = -\frac{2}{3} k \bar{u}_{k,k}$$

, S , C_i

Table 2.4

(2.42)

(2.43)

\mathbf{e}

(2.43)

(production of

dissipation)

C_1 C_4

, $C_1 = 2$ $C_4 = 1$

(2.44)

1

2

(return-to-equilibrium) ,

. Wu et al.

$$C_5 = -1.1,$$

$$C_{6,ISO} = -0.5, C_{6,AXI} = -2 .$$

Table 2.4 The values of the model constants in the $k - \mathbf{e} - \mathbf{t}$ model

C_1	2.0
C_4	1.0
C_5	-1.1
$C_{6,ISO}$	-0.5 (for isotropic compression flow)
$C_{6,AXI}$	-2.0 (for axisymmetric expansion flow)

$k - \mathbf{e} - \mathbf{t}$

Wu et al.가

$$\frac{dR_{ij}}{dt} = P_{ij} + T_{ij}^{(1)} - \mathbf{e}\mathbf{f}_{ij} - \frac{2}{3}\mathbf{e}\mathbf{d}_{ij} \quad (2.45)$$

P_{ij} production tensor

$$P_{ij} = -(R_{ik}S_{kj} + R_{jk}S_{ki}) + (R_{ik}\Omega_{kj} + R_{jk}\Omega_{ki}) \quad (2.46)$$

(mean strain rate tensor) S_{ij}

(mean

rotation tensor) Ω_{ij}

$$S_{ij} = \frac{1}{2}(\bar{u}_{i,j} + \bar{u}_{j,i}) \quad (2.47)$$

$$\Omega_{ij} = \frac{1}{2}(\bar{u}_{i,j} - \bar{u}_{j,i}) \quad (2.48)$$

$$T_{ij}^{(1)}$$

$$\begin{aligned} T_{ij}^{(1)} = q^2 \left\{ \frac{2}{5} S_{ij} - \frac{2}{15} S_{kk} \mathbf{d}_{ij} + 4A_1 S_{kk} b_{ij} \right. \\ \left. - 6A_1 \left(b_{ik} S_{kj} + b_{jk} S_{ki} - \frac{2}{3} b_{nm} S_{nm} \mathbf{d}_{ij} \right) \right. \\ \left. - \left(\frac{4}{3} + \frac{14}{3} A_1 \right) (b_{ik} \Omega_{kj} + b_{jk} \Omega_{ki}) \right\} \end{aligned} \quad (2.49)$$

$$\left. \begin{aligned} A_1 = -0.34 + 0.12 \exp \left(-0.3 \frac{P_{INC}}{\mathbf{e}} \right) \\ b_{ij} = \frac{R_{ij}}{R_{kk}} - \frac{\mathbf{d}_{ij}}{3} \end{aligned} \right\} \quad (2.50)$$

$$\left. \begin{aligned} \mathbf{f}_{ij} = A_0 b_{ij} \\ A_0 = 1 \end{aligned} \right\} \quad (2.51)$$

가 ,

$k - \mathbf{e} - \mathbf{t}$

3.

3.1

Fig.3.1

, \mathbf{x} r

, Fig.3.2

(2.25)

가

. \mathbf{f}

P(Fig.3.2)

[48].

$$\frac{1}{\mathbf{d}} \int_t^{t+dt} \left\{ \int_{\mathbf{x}_w}^{\mathbf{x}_e} \int_{r_s}^{r_n} (\mathbf{r} z_p \mathbf{f}) r dr d\mathbf{x} + \int_{r_s}^{r_n} \left[\mathbf{n} \hat{\mathbf{u}} \mathbf{f} - \frac{\Gamma_f}{z_p} \frac{\mathcal{J}[\mathbf{f}]}{\mathcal{J}[\mathbf{x}]} \right]_{\mathbf{x}_w}^{\mathbf{x}_e} r dr \right. \quad (3.1)$$

$$\left. + \int_{\mathbf{x}_w}^{\mathbf{x}_e} \left[r \mathbf{r} \mathbf{v} \mathbf{f} - r \Gamma_f \frac{\mathcal{J}[\mathbf{f}]}{\mathcal{J}[\mathbf{r}]} \right]_{r_s}^{r_n} z_p d\mathbf{x} - \int_{\mathbf{x}_w}^{\mathbf{x}_e} \int_{r_s}^{r_n} (S_f)_{\mathbf{x},r} z_p r dr d\mathbf{x} \right\} dt = 0$$

1

$$\frac{1}{\mathbf{d}} \int_t^{t+dt} \left(\int_{\mathbf{x}_w}^{\mathbf{x}_e} \int_{r_s}^{r_n} (\mathbf{r} z_p \mathbf{f}) r dr d\mathbf{x} \right) dt = \frac{(\mathbf{r} \mathbf{f})_p^n v_p^n - (\mathbf{r} \mathbf{f})_p^o v_p^o}{\mathbf{d}} \quad (3.2)$$

$$v_p = \int_{\mathbf{x}_w}^{\mathbf{x}_e} \int_{r_s}^{r_n} z_p r dr d\mathbf{x} = \frac{1}{2} z_p (r_n^2 - r_s^2) (\mathbf{x}_e - \mathbf{x}_w) \quad (3.3)$$

'n'

'o'

'new'

'old'

,

\mathbf{d}

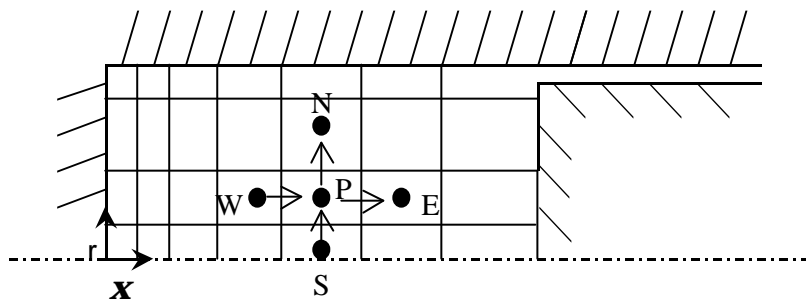


Fig.3.1 Grid structure and its notation

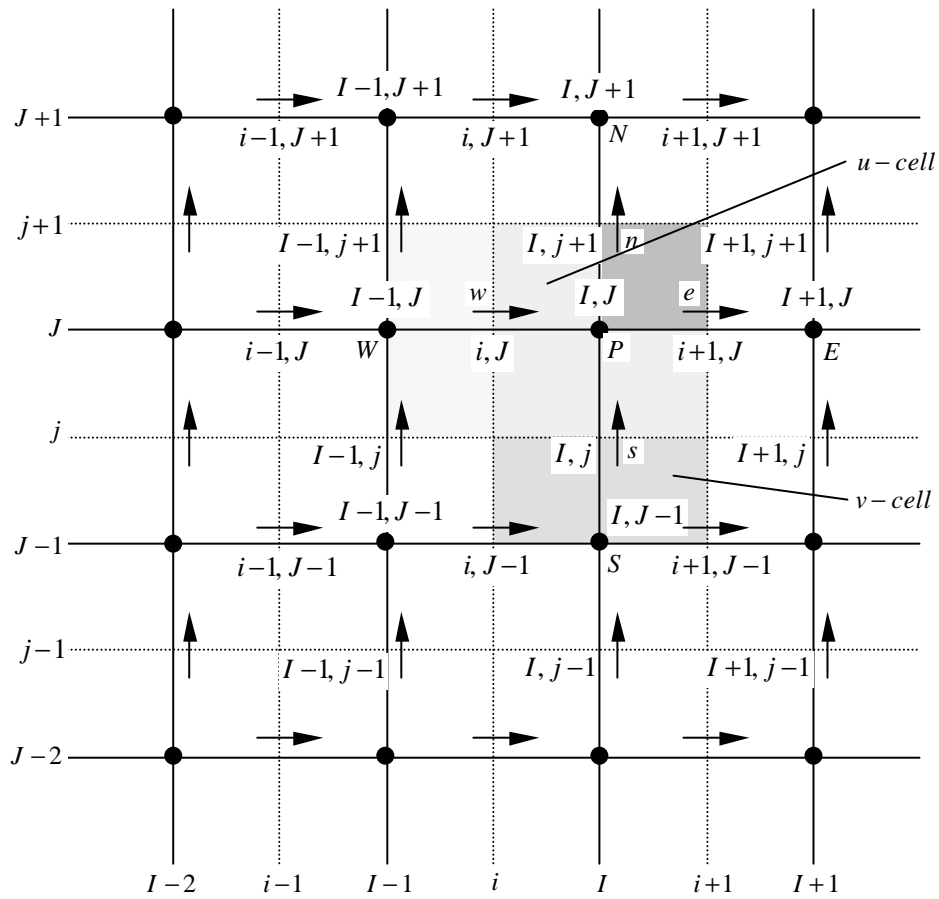


Fig.3.2 Control volume and its notation

f

$$\begin{aligned}
 F_x &= \int_{r_s}^{r_n} \left[\mathbf{r}\hat{u}\mathbf{f} - \frac{\Gamma_f}{z_p} \frac{\mathbf{f}}{\mathbf{x}} \right]_w^e r dr \\
 &= (\mathbf{r}\hat{u}a)_e \left(\mathbf{f}_e - \frac{\mathbf{f}_E - \mathbf{f}_P}{Pe_e} \right) - (\mathbf{r}\hat{u}a)_w \left(\mathbf{f}_w - \frac{\mathbf{f}_P - \mathbf{f}_W}{Pe_w} \right) \\
 a &= \left(\frac{r_n^2 - r_s^2}{2} \right), \quad Pe_e \quad Pe_w
 \end{aligned} \tag{3.4}$$

Peclet

$$\begin{aligned}
 Pe_e &= \frac{(\mathbf{r}\hat{u})_e}{\frac{\Gamma_{f_e}}{z_p} \mathbf{d}\mathbf{x}_{EP}} \\
 Pe_w &= \frac{(\mathbf{r}\hat{u})_w}{\frac{\Gamma_{f_w}}{z_p} \mathbf{d}\mathbf{x}_{PW}}
 \end{aligned} \tag{3.5}$$

'e' 'w' **r** Γ_f W, P

E

$$\begin{aligned}
 \mathbf{f}_e &= \frac{\mathbf{f}_E - \mathbf{f}_P}{Pe_e} = (1 - \mathbf{a}_e) \mathbf{f}_E + \mathbf{a}_e \mathbf{f}_P \\
 \mathbf{f}_w &= \frac{\mathbf{f}_P - \mathbf{f}_W}{Pe_w} = \mathbf{a}_w \mathbf{f}_W + (1 - \mathbf{a}_w) \mathbf{f}_P
 \end{aligned} \tag{3.6}$$

a Peclet

, Peclet

$$\mathbf{a} = \begin{cases} \frac{1}{2} + \frac{1}{Pe} & |Pe| \leq 2 \\ 1 & Pe > 2 \\ 0 & Pe < -2 \end{cases}$$

(3.1)

$$\begin{aligned} & \frac{1}{\mathbf{d}} \int_t^{t+\mathbf{d}} \int_{r_s}^{r_n} \left[\mathbf{r} \hat{u} \mathbf{f} - \frac{\Gamma_f}{z_p} \frac{\mathcal{J}[\mathbf{f}]}{\mathcal{J}[\mathbf{x}]} \right]_{x_w}^{x_e} r dr dt \\ & = (\mathbf{r} \hat{u} a)_e [(1 - \mathbf{a}_e) \mathbf{f}_E + \mathbf{a}_e \mathbf{f}_P] - (\mathbf{r} \hat{u} a)_w [\mathbf{a}_w \mathbf{f}_W + (1 - \mathbf{a}_w) \mathbf{f}_P] \end{aligned} \quad (3.7)$$

$$\begin{aligned} & \frac{1}{\mathbf{d}} \int_t^{t+\mathbf{d}} \int_{x_w}^{x_e} \left[r \mathbf{r} v \mathbf{f} - r \Gamma_f \frac{\mathcal{J}[\mathbf{f}]}{\mathcal{J}[\mathbf{r}]} \right]_{r_s}^{r_n} z_p d\mathbf{x} dt \\ & = (\mathbf{r} v a)_n [(1 - \mathbf{a}_n) \mathbf{f}_N + \mathbf{a}_n \mathbf{f}_P] - (\mathbf{r} v a)_s [\mathbf{a}_s \mathbf{f}_S + (1 - \mathbf{a}_s) \mathbf{f}_P] \end{aligned} \quad (3.8)$$

(3.1)

$$\frac{1}{\mathbf{d}} \int_t^{t+\mathbf{d}} \int_{v_p}^{v_e} (S_f)_{x,r} dv dt = S_p \mathbf{f}_p + S_u \quad (3.9)$$

$$S_p \quad S_u \quad \mathbf{f}$$

(3.1)

$$\frac{(\mathbf{r} v)_p^n - (\mathbf{r} v)_p^o}{\mathbf{d}} + (\mathbf{r} \hat{u} a)_e^n - (\mathbf{r} \hat{u} a)_w^n + (\mathbf{r} v a)_n^n - (\mathbf{r} v a)_s^n = 0 \quad (3.10)$$

가 ,

$$\begin{aligned}
& \frac{(\mathbf{r}_p)^o [\mathbf{f}_p - \mathbf{f}_p^o]}{\mathbf{d}} + \mathbf{r}_e^n [(1 - \mathbf{a}_e)(\mathbf{f}_E - \mathbf{f}_p)]^n \\
& + \mathbf{r}_w^n [\mathbf{a}_w(\mathbf{f}_p - \mathbf{f}_w)]^n + \mathbf{r}_n^n [(1 - \mathbf{a}_n)(\mathbf{f}_N - \mathbf{f}_p)]^n \\
& + \mathbf{r}_s^n [\mathbf{a}_s(\mathbf{f}_p - \mathbf{f}_s)]^n - S_p \mathbf{f}_p - S_u = 0
\end{aligned} \tag{3.11}$$

$$\mathbf{r}_e^n \equiv (\mathbf{r}_e \hat{u}_e a_e)^n, \quad \mathbf{r}_n^n \equiv (\mathbf{r}_n v_n a_n)^n$$

$$\begin{aligned}
\mathbf{r}_e &= [\mathbf{r}_p f_1 + \mathbf{r}_E (1 - f_1)] a_e \hat{u}_e \\
\mathbf{r}_n &= [\mathbf{r}_p f_2 + \mathbf{r}_N (1 - f_2)] a_n v_n
\end{aligned} \tag{3.12}$$

$$f_1 \quad f_2 \quad \text{(factor)}$$

$$\begin{aligned}
f_1 &= \frac{\mathbf{d} \mathbf{E}_e}{\mathbf{d} \mathbf{E}_p} \\
f_2 &= \frac{\mathbf{d} N_n}{\mathbf{d} N_p}
\end{aligned} \tag{3.13}$$

(3.11)

$$(A_p - S_p) \mathbf{f}_p = \sum_c A_c \mathbf{f}_c + A_p^o \mathbf{f}_p + S_u \tag{3.14}$$

$$A_p = \sum_c A_c + A_p^o \tag{3.15}$$

$$\sum_c \quad \text{N, S, E, W}$$

$$\begin{aligned}
A_E &= m_e^n (a_e^n - 1) \\
A_W &= m_w^n a_w^n \\
A_N &= m_n^n (a_n^n - 1) \\
A_S &= m_s^n a_s^n \\
A_p^o &= \frac{r_p^o v_p^o}{t}
\end{aligned}
\tag{3.16}$$

(3.14) (3.16)

(3.16)

Fig.3.2

3.2

3.2

3.2.1

[54]

Harlow Welch가

(staggered grid)

가
 ,
 ,
 .
 가
 .
 ,
 ,
 .

Fig.3.3 Fig.3.4 u v

Fig.3.3 u Fig.3.2
 (I, J) I , Fig.3.4 v
 J ,

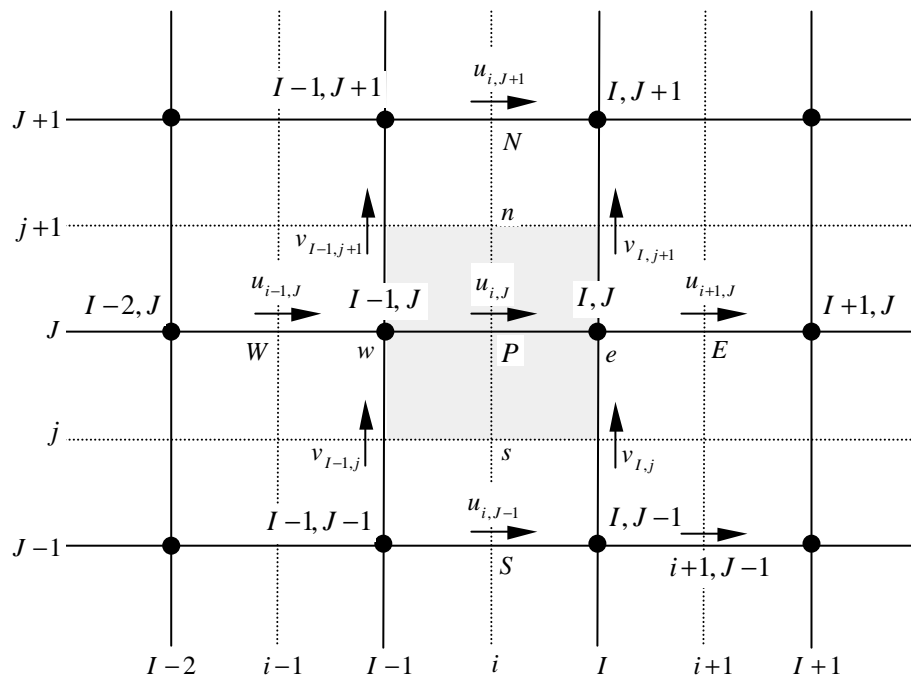


Fig.3.3 u -control volume and its neighbouring velocity components

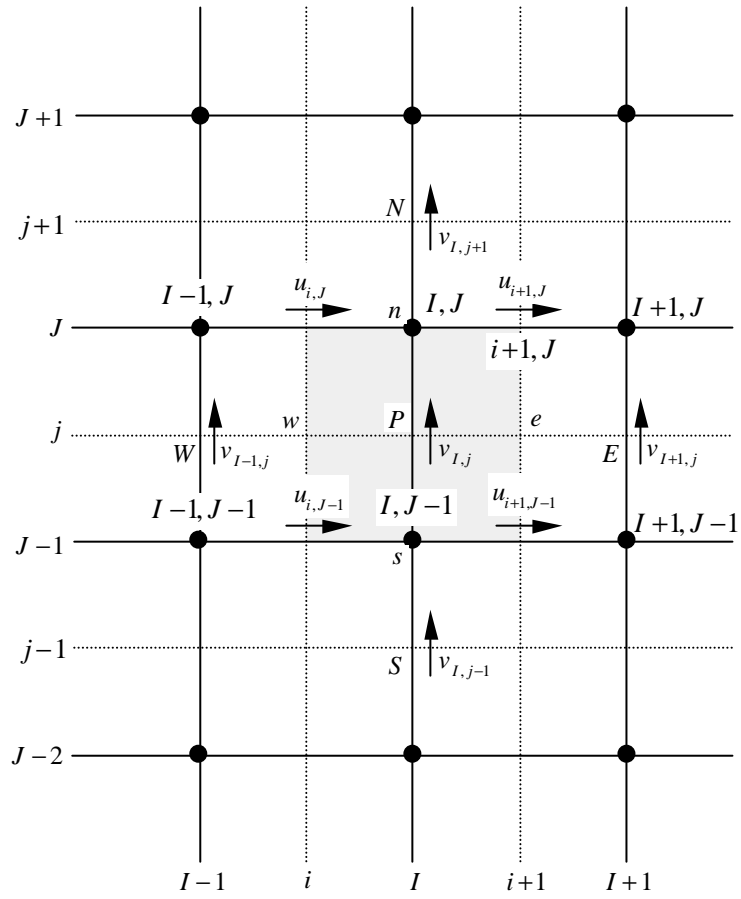


Fig. 3.4 v -control volume and its neighbouring velocity components

Fig.3.3 Fig.3.4

u v

$$a_{i,j}u_{i,j} = \sum a_{nb}u_{nb} + (p_{i-1,j} - p_{i,j})A_{i,j} + b_{i,j} \quad (3.17)$$

$$a_{i,j}v_{i,j} = \sum a_{nb}v_{nb} + (p_{i,j-1} - p_{i,j})A_{i,j} + b_{i,j} \quad (3.18)$$

$$b_{i,j}, b_{i,j}, \quad , A_{i,j}, A_{i,j}$$

$$\sum a_{nb}u_{nb} \quad (i-1, J), (i+1, J), (i, J+1) \quad (i, J-1)$$

p 가 (3.17) (3.18)

3.2.2 SIMPLE

SIMPLE(Semi-Implicit Method for Pressure Linked Equations)

Patankar Spalding^[55]

(guess and correct)

. SIMPLE

$$p^*$$

$$(3.17) \quad (3.18)$$

$$u^* \quad v^*$$

$$a_{i,j} u_{i,j}^* = \sum a_{nb} u_{nb}^* + (p_{I-1,j}^* - p_{I,j}^*) A_{i,j} + b_{i,j} \quad (3.19)$$

$$a_{I,j} v_{I,j}^* = \sum a_{nb} v_{nb}^* + (p_{I,j-1}^* - p_{I,j}^*) A_{I,j} + b_{I,j} \quad (3.20)$$

p p^* (pressure
correction) p'

$$p = p^* + p' \quad (3.21)$$

u, v u^*, v^*

u', v'

$$u = u^* + u' \quad (3.22)$$

$$v = v^* + v' \quad (3.23)$$

p u, v

(3.17) (3.18) (3.19) (3.20)

$$a_{i,j} (u_{i,j} - u_{i,j}^*) = \sum a_{nb} (u_{nb} - u_{nb}^*) + \{ (p_{I-1,j} - p_{I-1,j}^*) - (p_{I,j} - p_{I,j}^*) \} A_{i,j} \quad (3.24)$$

$$a_{I,j} (v_{I,j} - v_{I,j}^*) = \sum a_{nb} (v_{nb} - v_{nb}^*) + \{ (p_{I,j-1} - p_{I,j-1}^*) - (p_{I,j} - p_{I,j}^*) \} A_{I,j} \quad (3.25)$$

(3.21) ~ (3.23) (3.24) (3.25)

$$a_{i,j} u'_{i,j} = \sum a_{nb} u'_{nb} + (p'_{I-1,j} - p'_{I,j}) A_{i,j} \quad (3.26)$$

$$a_{I,j} v'_{I,j} = \sum a_{nb} v'_{nb} + (p'_{I,J-1} - p'_{I,J}) A_{I,j} \quad (3.27)$$

(3.26) (3.27)

$$\sum a_{nb} u'_{nb}$$

$$\sum a_{nb} v'_{nb}$$

SIMPLE

(main approximation)

implicit)

(3.26) (3.27)

$$u'_{i,j} = d_{i,j} (p'_{I-1,J} - p'_{I,J}) \quad (3.28)$$

$$v'_{I,j} = d_{I,j} (p'_{I,J-1} - p'_{I,J}) \quad (3.29)$$

$$d_{i,j} = \frac{A_{i,J}}{a_{i,j}}, \quad d_{I,j} = \frac{A_{I,j}}{a_{I,j}} \quad (3.30)$$

(3.28) (3.29) (3.22) (3.23)

$$u_{i,j} = u_{i,j}^* + d_{i,j} (p'_{I-1,J} - p'_{I,J}) \quad (3.31)$$

$$v_{I,j} = v_{I,j}^* + d_{I,j} (p'_{I,J-1} - p'_{I,J}) \quad (3.32)$$

$u_{i+1,J}$ $v_{I,j+1}$

$$u_{i+1,J} = u_{i+1,J}^* + d_{i+1,J} (p'_{I,J} - p'_{I+1,J}) \quad (3.33)$$

$$v_{I,j+1} = v_{I,j+1}^* + d_{I,j+1} (p'_{I,J} - p'_{I,J+1}) \quad (3.34)$$

$$d_{i+1,J} = \frac{A_{i+1,J}}{a_{i+1,J}} \quad , \quad d_{I,j+1} = \frac{A_{I,j+1}}{a_{I,j+1}} \quad (3.35)$$

Fig.3.5

$$\{(\mathbf{ru}A)_{i+1,J} - (\mathbf{ru}A)_{i,J}\} + \{(\mathbf{rv}A)_{I,j+1} - (\mathbf{rv}A)_{I,j}\} = 0 \quad (3.36)$$

$$(3.31) \sim (3.34) \quad (3.36)$$

$$\begin{aligned} & \left[\mathbf{r}_{i+1,J} A_{i+1,J} \{u_{i+1,J}^* + d_{i+1,J} (p'_{I,J} - p'_{I+1,J})\} \right. \\ & \quad \left. - \mathbf{r}_{i,J} A_{i,J} \{u_{i,J}^* + d_{i,J} (p'_{I-1,J} - p'_{I,J})\} \right] \\ & + \left[\mathbf{r}_{I,j+1} A_{I,j+1} \{v_{I,j+1}^* + d_{I,j+1} (p'_{I,J} - p'_{I,J+1})\} \right. \\ & \quad \left. - \mathbf{r}_{I,j} A_{I,j} \{v_{I,j}^* + d_{I,j} (p'_{I,J-1} - p'_{I,J})\} \right] = 0 \end{aligned} \quad (3.37)$$

$$\begin{aligned} & [(\mathbf{rd}A)_{i+1,J} + (\mathbf{rd}A)_{i,J} + (\mathbf{rd}A)_{I,j+1} + (\mathbf{rd}A)_{I,j}] p'_{I,J} \\ & = (\mathbf{rd}A)_{i+1,J} p'_{I+1,J} + (\mathbf{rd}A)_{i,J} p'_{I-1,J} \\ & \quad + (\mathbf{rd}A)_{I,j+1} p'_{I,J+1} + (\mathbf{rd}A)_{I,j} p'_{I,J-1} \\ & \quad + [(\mathbf{ru}^*A)_{i,J} - (\mathbf{ru}^*A)_{i+1,J} + (\mathbf{rv}^*A)_{I,j} - (\mathbf{rv}^*A)_{I,j+1}] \end{aligned} \quad (3.38)$$

p'

$$\begin{aligned} a_{I,J} p'_{I,J} & = a_{I+1,J} p'_{I+1,J} + a_{I-1,J} p'_{I-1,J} + a_{I,J+1} p'_{I,J+1} \\ & \quad + a_{I,J-1} p'_{I,J-1} + b'_{I,J} \end{aligned} \quad (3.39)$$

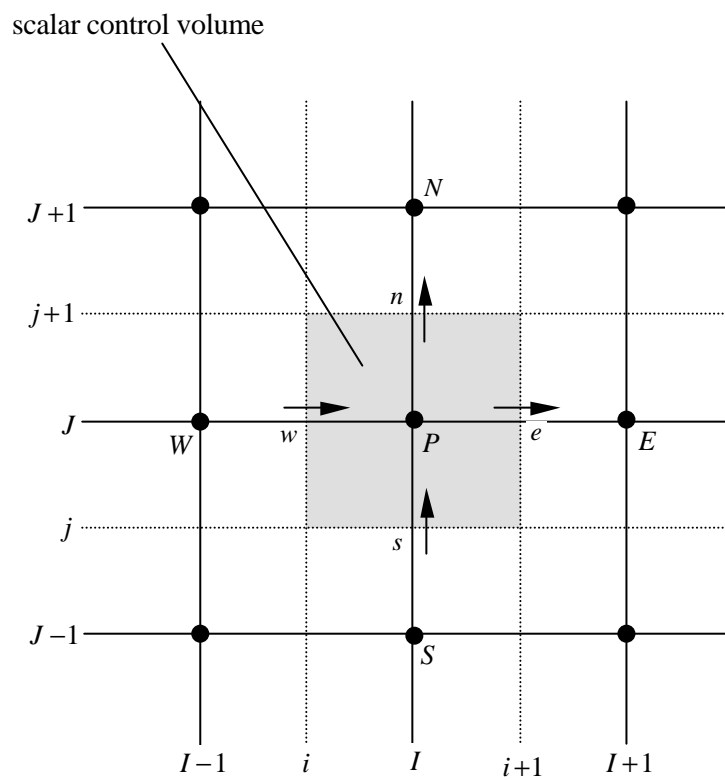


Fig.3.5 The scalar control volume used for the discretization of the continuity equation

$$a_{I,J} = a_{I+1,J} + a_{I-1,J} + a_{I,J+1} + a_{I,J-1}$$

$$a_{I+1,J} = (\mathbf{rl}A)_{i+1,J}$$

$$a_{I-1,J} = (\mathbf{rl}A)_{i,J}$$

$$a_{I,J+1} = (\mathbf{rl}A)_{I,j+1}$$

$$a_{I,J-1} = (\mathbf{rl}A)_{I,j}$$

$$b'_{I,J} = (\mathbf{ru}^*A)_{i,j} - (\mathbf{ru}^*A)_{i+1,j} + (\mathbf{rv}^*A)_{I,j} - (\mathbf{rv}^*A)_{I,j+1}$$

(3.39)

p'

b'

u^*, v^*

(3.39)

,

p'

p'

(3.21)

,

(3.31) ~ (3.34)

$$\sum a_{nb} u'_{nb}$$

$$p^* = p, \quad u^* = u, \quad v^* = v$$

0

(under relaxation)

p^{new}

$$p^{new} = p^* + \mathbf{a}_p p' \quad (3.40)$$

\mathbf{a}_p 가 1 이고 p^* 가 p' 이면 p^{new} 가 p' 가 된다. \mathbf{a}_p 가 0 이면 p^{new} 가 p^* 가 된다. \mathbf{a}_p 가 0 과 1 사이이면 p^{new} 가 p^* 와 p' 사이의 값이 된다.

$$u^{new} = \mathbf{a}_u u + (1 - \mathbf{a}_u) u^{(n-1)} \quad (3.41)$$

$$v^{new} = \mathbf{a}_v v + (1 - \mathbf{a}_v) v^{(n-1)} \quad (3.42)$$

\mathbf{a}_u 와 \mathbf{a}_v 가 0 이면 u^{new} 와 v^{new} 가 각각 $u^{(n-1)}$ 와 $v^{(n-1)}$ 가 된다. \mathbf{a}_u 와 \mathbf{a}_v 가 1 이면 u^{new} 와 v^{new} 가 각각 u 와 v 가 된다.

$$\frac{a_{i,J}}{\mathbf{a}_u} u_{i,J} = \sum a_{nb} u_{nb} + (p_{I-1,J} - p_{I,J}) A_{i,J} + b_{i,J} + \left\{ (1 - \mathbf{a}_u) \frac{a_{i,J}}{\mathbf{a}_u} \right\} u_{i,J}^{(n-1)} \quad (3.43)$$

v -

$$\frac{a_{I,j}}{\mathbf{a}_v} v_{I,j} = \sum a_{nb} v_{nb} + (p_{I,J-1} - p_{I,J}) A_{I,j} + b_{I,j} + \left\{ (1 - \mathbf{a}_v) \frac{a_{I,j}}{\mathbf{a}_v} \right\} v_{I,j}^{(n-1)} \quad (3.44)$$

d -

$$d_{i,j} = \frac{A_{i,j} \mathbf{a}_u}{a_{i,j}}$$

$$d_{i+1,j} = \frac{A_{i+1,j} \mathbf{a}_u}{a_{i+1,j}}$$

$$d_{I,j} = \frac{A_{I,j} \mathbf{a}_v}{a_{I,j}}$$

$$d_{I,j+1} = \frac{A_{I,j+1} \mathbf{a}_v}{a_{I,j+1}}$$

SIMPLE

. SIMPLE

Fig.3.6

SIMPLE

, CFD

SIMPLE

p'

Implicit with Splitting of Operators)

SIMPLER(SIMPLE Revised), PISO(Pressure

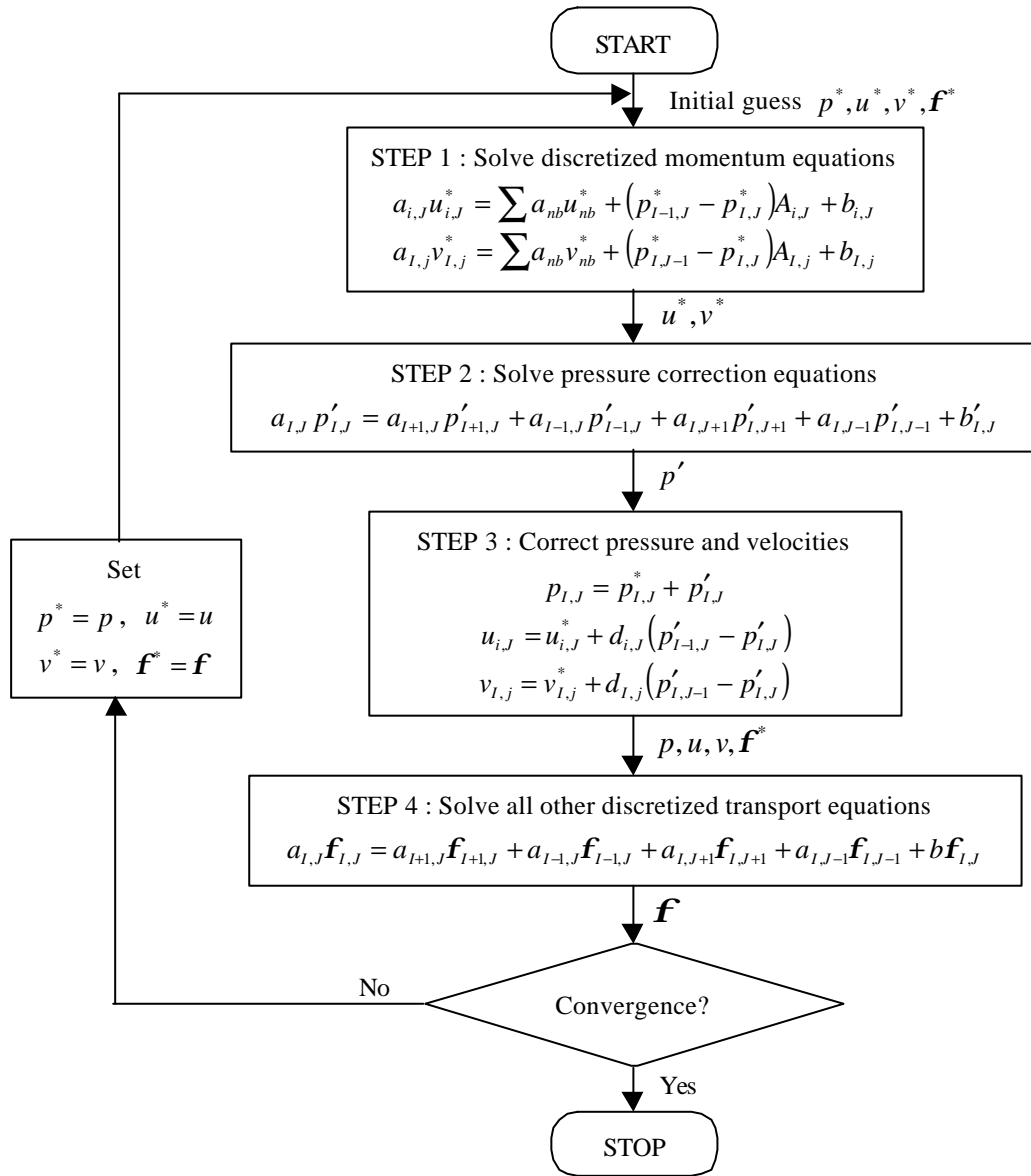


Fig.3.6 The SIMPLE algorithm

3.2.3 PISO

PISO - Issa^[56]가 , 1
 (predictor step) 2 (corrector step) ,
 가
 가
 . PISO SIMPLE

1)

SIMPLE p^* 가 (3.19), (3.20)
 u^*, v^* .

2) 1

u^*, v^* p^* 가
 u^{**}, v^{**}

SIMPLE 1 . SIMPLE
 (3.28), (3.29) , PISO

가

$$p^{**} = p^* + p'$$

$$u^{**} = u^* + u'$$

$$v^{**} = v^* + v'$$

u^{**} v^{**} .

$$u_{i,j}^{**} = u_{i,j}^* + d_{i,j} (p'_{l-1,j} - p'_{l,j}) \quad (3.45)$$

$$v_{I,j}^{**} = v_{I,j}^* + d_{I,j} (p'_{I,J-1} - p'_{I,J}) \quad (3.46)$$

SIMPLE (3.45) (3.46)

(3.26) (3.39) . PISO

$$(3.39) \quad 1 \quad , \quad 1 \quad p' \quad u^{**} \quad v^{**} \quad (3.45)$$

(3.46)

3) 2

SIMPLE , PISO

. u^{**} v^{**}

$$a_{i,j} u_{i,j}^{**} = \sum a_{nb} u_{nb}^* + (p_{I-1,J}^{**} - p_{I,J}^{**}) A_{i,j} + b_{i,j} \quad (3.47)$$

$$a_{I,j} v_{I,j}^{**} = \sum a_{nb} v_{nb}^* + (p_{I,J-1}^{**} - p_{I,J}^{**}) A_{I,j} + b_{I,j} \quad (3.48)$$

. 2 u^{***} v^{***}

$$a_{i,j} u_{i,j}^{***} = \sum a_{nb} u_{nb}^{**} + (p_{I-1,J}^{***} - p_{I,J}^{***}) A_{i,j} + b_{i,j} \quad (3.49)$$

$$a_{I,j} v_{I,j}^{***} = \sum a_{nb} v_{nb}^{**} + (p_{I,J-1}^{***} - p_{I,J}^{***}) A_{I,j} + b_{I,j} \quad (3.50)$$

(3.49) (3.50) (3.19) (3.20)

$$u_{i,j}^{***} = u_{i,j}^{**} + \frac{\sum a_{nb} (u_{nb}^{**} - u_{nb}^*)}{a_{i,j}} + d_{i,j} (p_{I-1,J}'' - p_{I,J}'') \quad (3.51)$$

$$v_{I,j}^{***} = v_{I,j}^{**} + \frac{\sum a_{nb} (v_{nb}^{**} - v_{nb}^*)}{a_{I,j}} + d_{I,j} (p_{I,J-1}'' - p_{I,J}'') \quad (3.52)$$

$$p'' = 2p^{**} + p''' \quad (3.53)$$

$$u''' = v''' \quad (3.36)$$

$$a_{I,J} p''_{I,J} = a_{I+1,J} p''_{I+1,J} + a_{I-1,J} p''_{I-1,J} + a_{I,J+1} p''_{I,J+1} + a_{I,J-1} p''_{I,J-1} + b''_{I,J} \quad (3.54)$$

$$a_{I,J} = a_{I+1,J} + a_{I-1,J} + a_{I,J+1} + a_{I,J-1}$$

$$a_{I+1,J} = (\mathbf{r}A)_{i+1,J}$$

$$a_{I-1,J} = (\mathbf{r}A)_{i,J}$$

$$a_{I,J+1} = (\mathbf{r}A)_{I,j+1}$$

$$a_{I,J-1} = (\mathbf{r}A)_{I,j}$$

$$b''_{I,J} = \left(\frac{\mathbf{r}A}{a} \right)_{i,j} \sum a_{nb} (u_{nb}^{**} - u_{nb}^*) - \left(\frac{\mathbf{r}A}{a} \right)_{i+1,J} \sum a_{nb} (u_{nb}^{**} - u_{nb}^*) + \left(\frac{\mathbf{r}A}{a} \right)_{I,j} \sum a_{nb} (v_{nb}^{**} - v_{nb}^*) - \left(\frac{\mathbf{r}A}{a} \right)_{I,j+1} \sum a_{nb} (v_{nb}^{**} - v_{nb}^*) \quad (3.54)$$

$$\left[(\mathbf{r}u^{**} A)_{i,j} - (\mathbf{r}u^{**} A)_{i+1,J} + (\mathbf{r}v^{**} A)_{I,j} - (\mathbf{r}v^{**} A)_{I,j+1} \right]$$

$$u^{**} = v^{**} \quad \text{가} \quad 0 \quad .$$

$$2 \quad p'' \quad (3.54) \quad , 2$$

$$p^{***} = p^{**} + p'' = p^* + p' + p'' \quad (3.55)$$

$$2 \quad (3.51) \quad (3.52)$$

Fig.3.7 PISO

PISO 2 , 2

가

SIMPLE

Issa et al.^[57]

(laminar backward-facing step)

(bench-mark)

CPU time SIMPLE

PISO

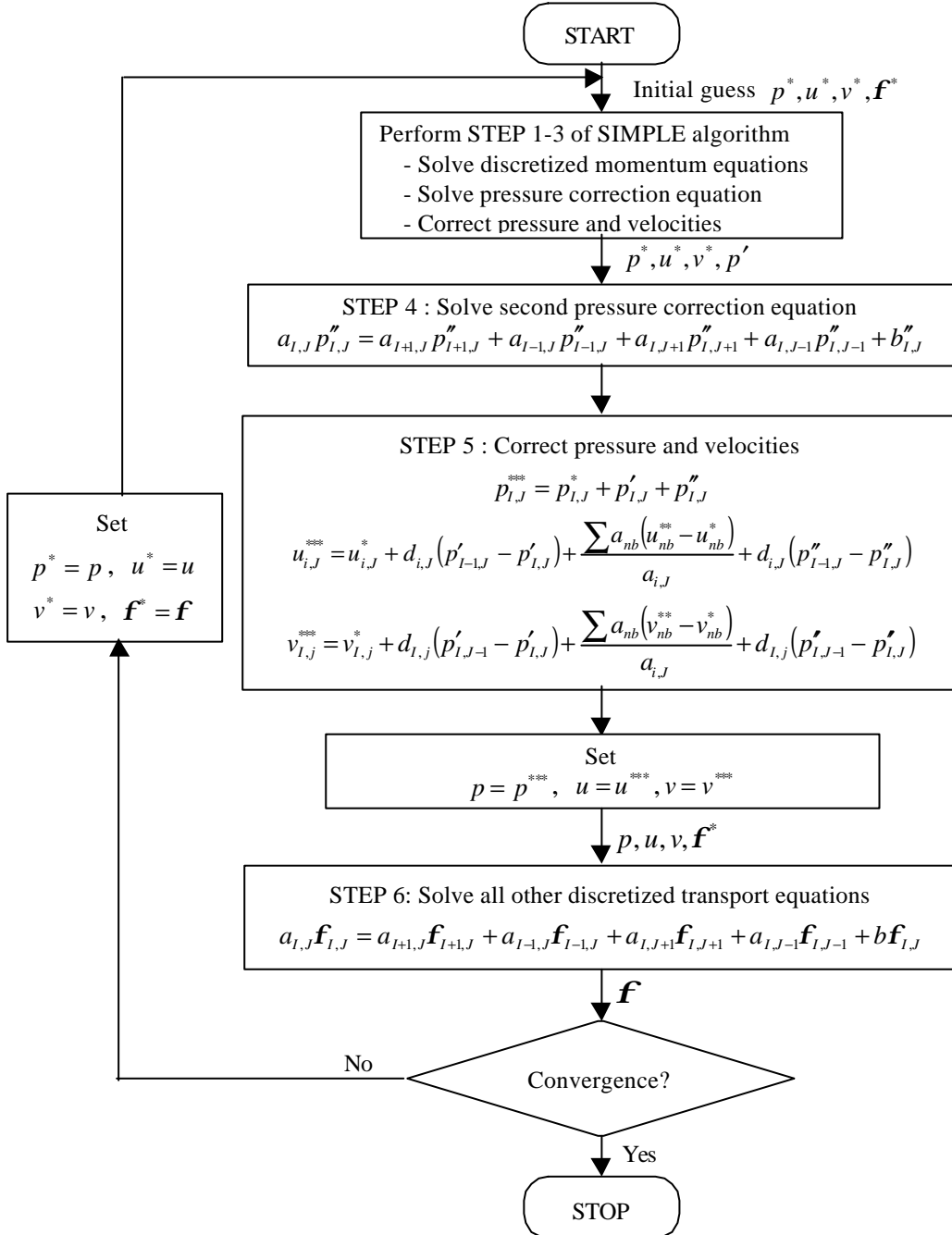


Fig.3.7 The PISO algorithm

3.3

(start-up)

가

1)

$$\left(\frac{\partial \mathbf{f}}{\partial r}\right)_{r=0} = 0 \quad (3.56)$$

0

2)

no-slip

0

u_p

(near-wall

value)

(wall function)

가

가

가

Patankar

and Spalding^[19]

Couette

1

3)

가

2

4.

4.1

4.1.1

Ahmadi-Befrui et al.^[47]

Table 4.1,

Fig. 4.1

75mm

200rpm

$\pm 0.5\%$. Fig. 4.1

34mm 가

Table 4.1 Geometric details of model engine^[14]

Bore	75 mm
Stroke	94 mm
Compression ratio	3.5
Connecting rod length	363.5 mm
Intake valve	
Diameter(D)	34.0 mm
Maximum lift(L)	7.3 mm
Dimensionless lift(L/D)	0.21
Seat angle	60°
Open at	6° BTDC
Close at	44° ABDC

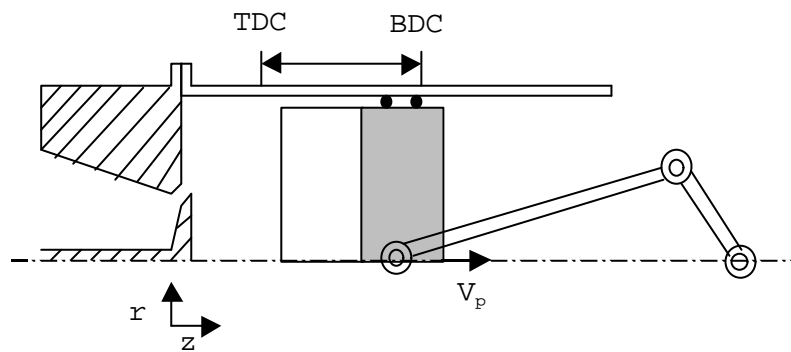


Fig 4.1 Diagram of piston-cylinder assembly

4.1.2

가 가
 가 가
 1
 (discharge coefficient) [58,59,60], Bicen et al.
 [61]

$$\begin{aligned}
 \frac{L_v}{D_v} < 0.052 & \quad C_D = \left(0.93 + 2.6923 \times \frac{L_v}{D_v} \right) \\
 0.052 \leq \frac{L_v}{D_v} < 0.113 & \quad C_D = \left(1.07 - 0.8623 \times \left(\frac{L_v}{D_v} - 0.052 \right) \right) \\
 0.113 \leq \frac{L_v}{D_v} < 0.2 & \quad C_D = \left(1.0174 + 0.9494 \times \left(\frac{L_v}{D_v} - 0.113 \right) \right) \\
 \frac{L_v}{D_v} \geq 0.2 & \quad C_D = \left(1.1 - 1.7 \times \left(\frac{L_v}{D_v} - 0.2 \right) \right)
 \end{aligned} \tag{4.1}$$

- 2
 가
 1) , (60°)
 2) V_{in} , k_{in} e_{in}

$$0.01V_{in}^2 \quad 3.65 \frac{k_{in}^{\frac{3}{2}}}{l} \quad [14] \quad l$$

[62]

4.2

Fig.4.2

[63]

40 x 40

60 x 60

1°

r

. z

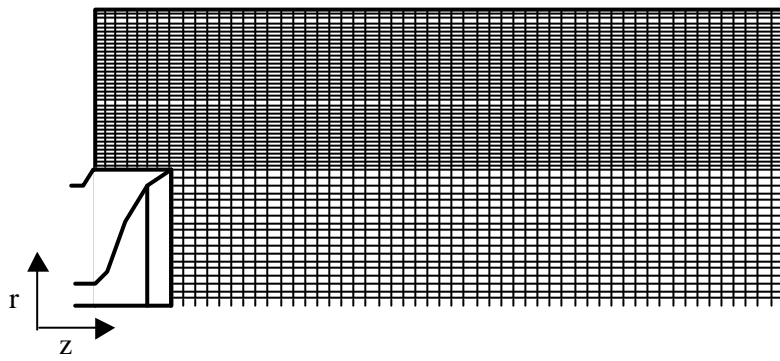


Fig.4.2 Grid structure for numerical calculation

4.3

Fig.4.3(a)~(f)

$$\bar{V}_p = 0.6267 \text{ ms}^{-1}$$

Ahmadi-Befrui et al.^[14]

$k - e$

$k - e - t$

15mm

Fig.4.3 (a) (c)

36° 90°

26mm

가

가

가

$k - e$

$k - e - t$

$k - e - t$

가

$k - e$

Fig.4.3 (b) (d)

36° 90°

90°

20mm

$k - e$

$k - e - t$

90°

$k - e - t$

가

$k - e$

270°

Fig.4.3 (e) (f)

$k - e$

$k - e - t$

$k - e - t$

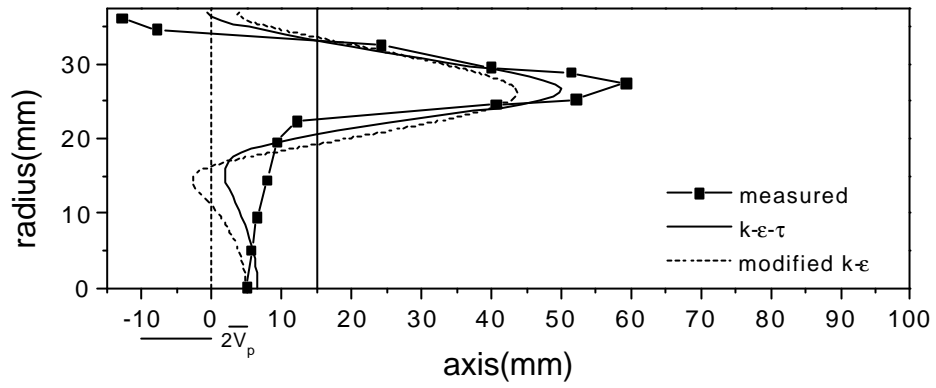
가

TDC

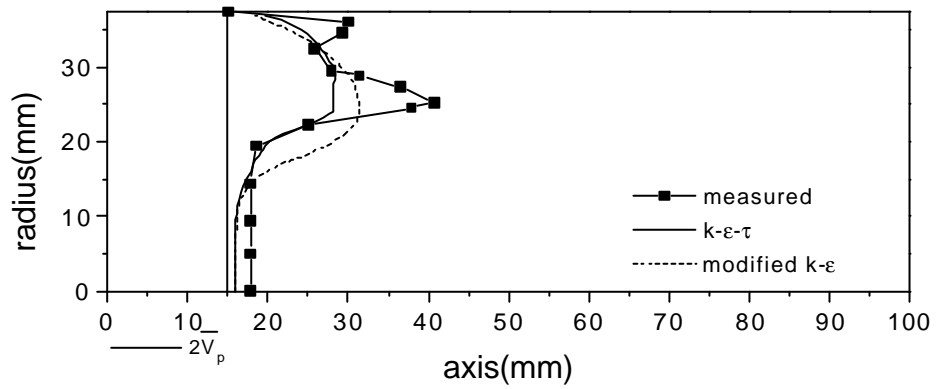
가

$k - e - t$

가



(a)

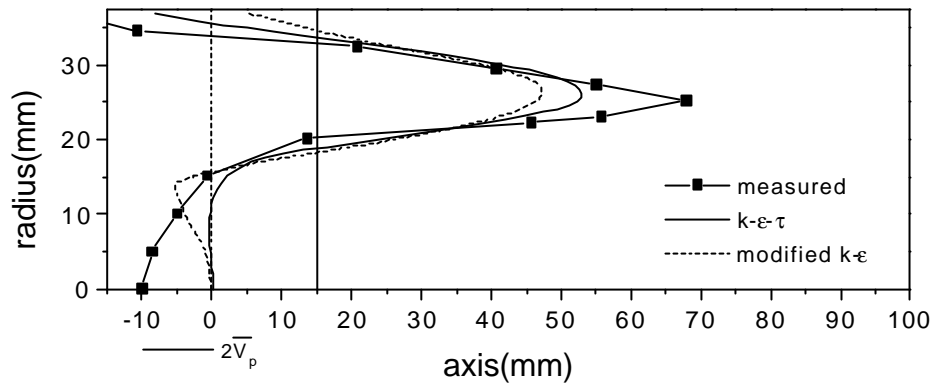


(b)

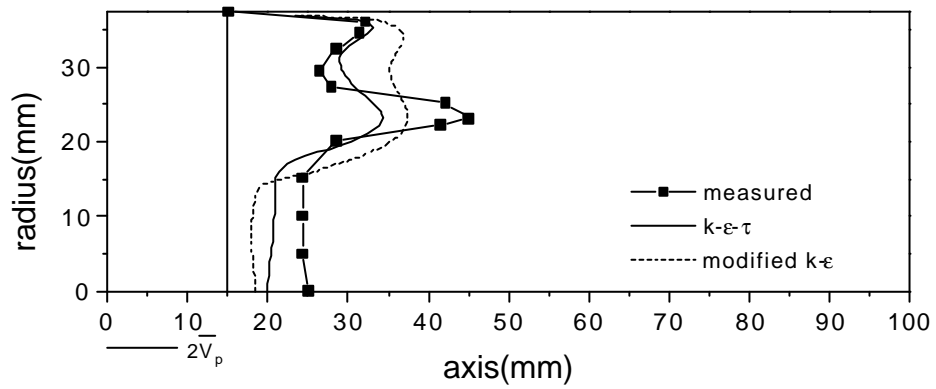
Fig.4.3 Radial profiles of axial mean velocity and rms velocity at $z=15\text{mm}$

(a) mean velocity at $q=36^\circ$

(b) rms velocity at $q=36^\circ$



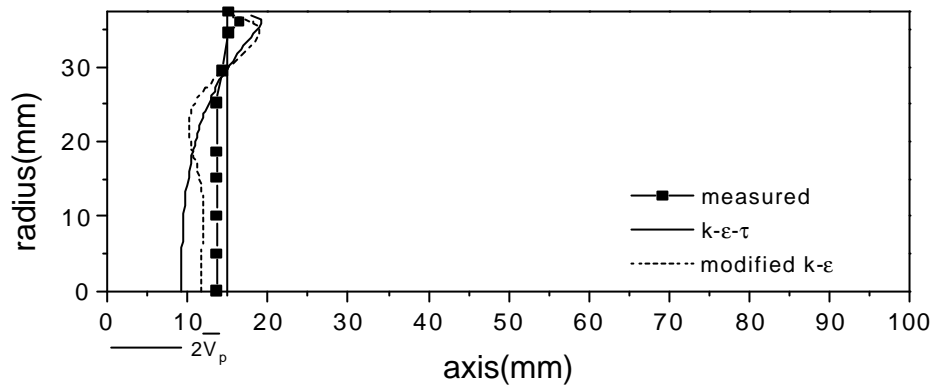
(c)



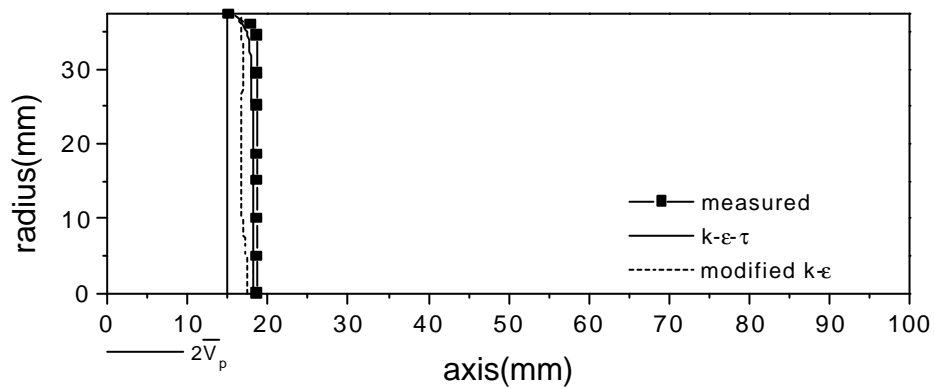
(d)

Fig.4.3 Radial profiles of axial mean velocity and rms velocity at $z=15\text{mm}$

(c) mean velocity at $\mathbf{q}=90^\circ$ (d) rms velocity at $\mathbf{q}=90^\circ$



(e)



(f)

Fig.4.3 Radial profiles of axial mean velocity and rms velocity at $z=15\text{mm}$

(e) mean velocity at $\mathbf{q}=270^\circ$ (f) rms velocity at $\mathbf{q}=270^\circ$

4.4

Fig.4.4 Fig.4.5 15mm,
25mm

[4] $k - \mathbf{e}$

, $k - \mathbf{e} - \mathbf{t}$

Fig.4.3 (a) (c) Fig.4.4 Fig.4.5 ,
(渦)

Fig.4.4 가 ,

, $10.5 \bar{V}_p$.

(main

vortex)가

가 .

, $k - \mathbf{e} - \mathbf{t}$

$k - \mathbf{e}$

Fig.4.5 가

가 . Fig.4.4 Fig.4.5

, $0.7\bar{V}_p$

. Fig.4.3(f)

. $k - \mathbf{e} - \mathbf{t}$

$k - \mathbf{e}$

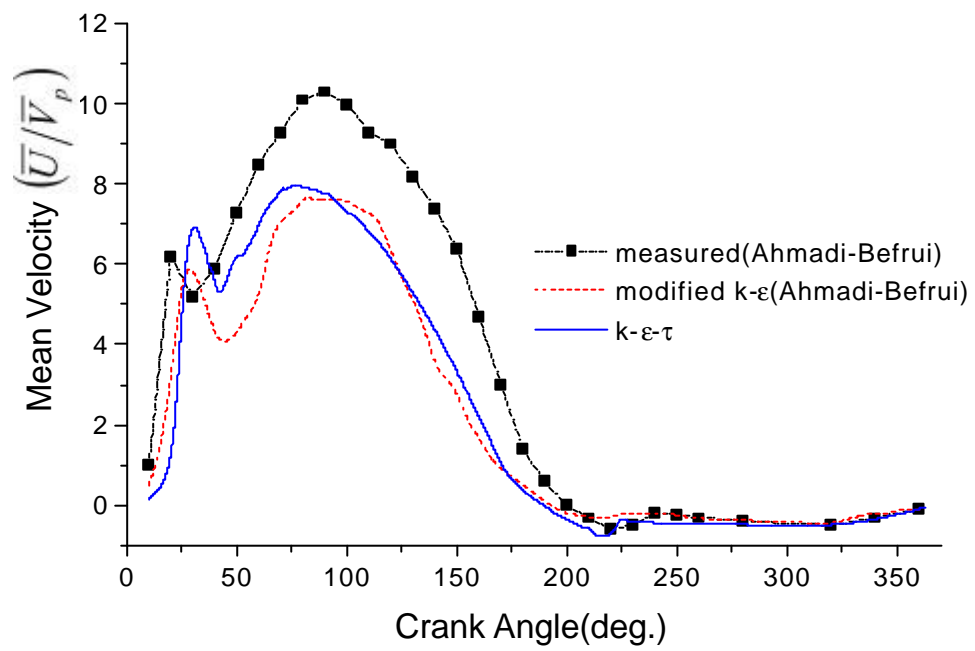


Fig.4.4 Temporal changes of axial mean velocity at $z=15\text{mm}$, $r=25\text{mm}$

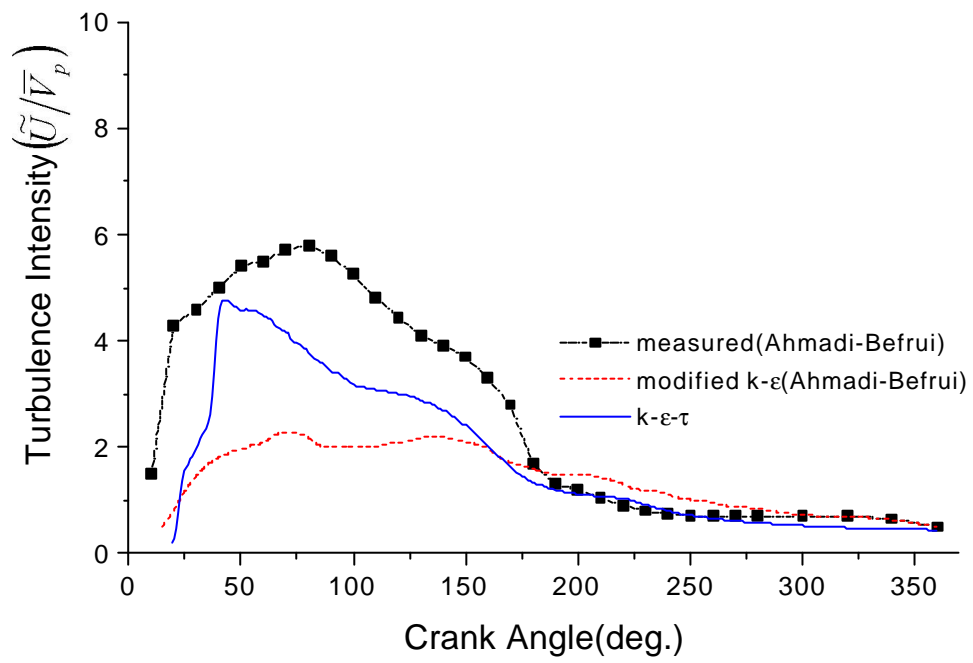


Fig.4.5 Temporal changes of turbulence intensity at $z=15\text{mm}$, $r=25\text{mm}$

4.5

$k - e$

$k - e - t$

, Fig.4.6 Fig.4.7

$$\sqrt{2k/3}/\bar{V}_p$$

Fig.4.6 (a) (b)

36°

가

가

가

가

Houtl^[64] 가

60°

가

Fig.4.6 (c) (d)

90°

가

가

가

가 ,
 180°(Fig.4.6 (e) (f))
 가

가 , 가
 [14.47]
 가
 가

36° 가
 가 ,
 90°
 $k - e$ $k - e - t$
 $k - e - t$
 가 $k - e$

180° . Fig.4.6 (g) (h) 가

225° ,

225°

가

Fig.4.6 (i) (j)

270°

가

, $k - e - t$

가 $k - e$

가

. Fig.4.6 (k)

(l)

Fig.4.7 (a)~(f)

가 가

Fig.4.7 (g)~(l)

$k - e - t$

가

$k - e$

Fig.4.7 (k) (l)

$k - e - t$

가 $k - e$

Fig.4.5 (b)

$k - e$

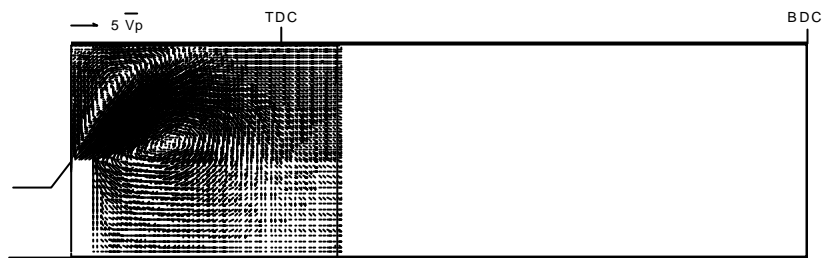
가

, $k - e - t$

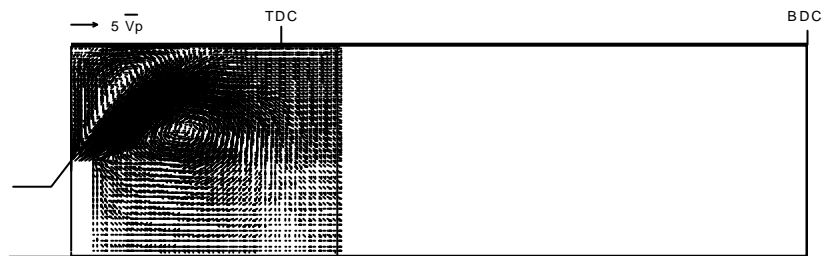
가 .

$k - e$

, $k - e - t$



(a)



(b)

Fig.4.6 Velocity fields of modified $k - e$ model and $k - e - t$ model
 (a) modified $k - e$ model, $q=36^\circ$ (b) $k - e - t$ model, $q=36^\circ$

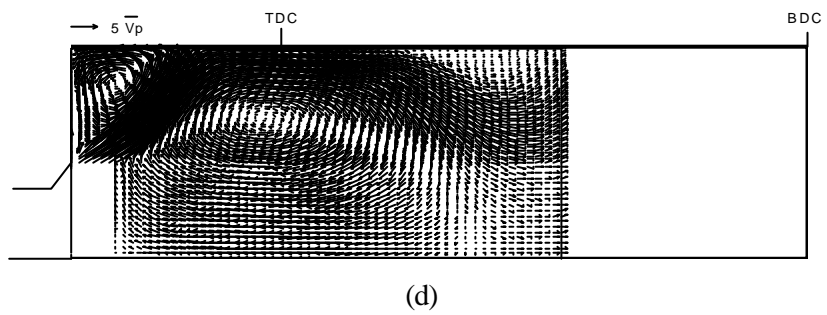
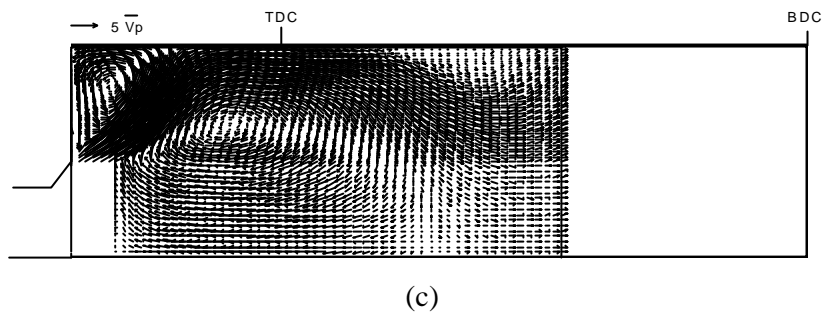
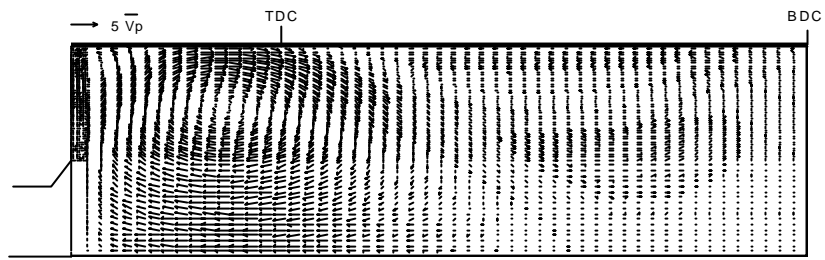
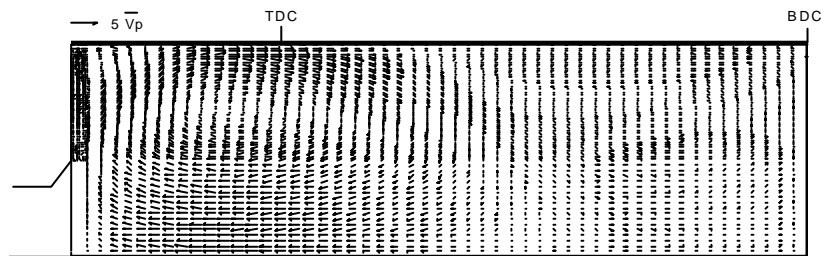


Fig.4.6 Velocity fields of modified $k - e$ model and $k - e - t$ model
 (c) modified $k - e$ model, $q=90^\circ$ (d) $k - e - t$ model, $q=90^\circ$

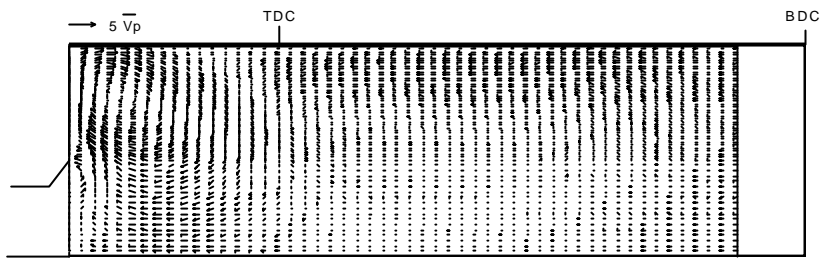


(e)

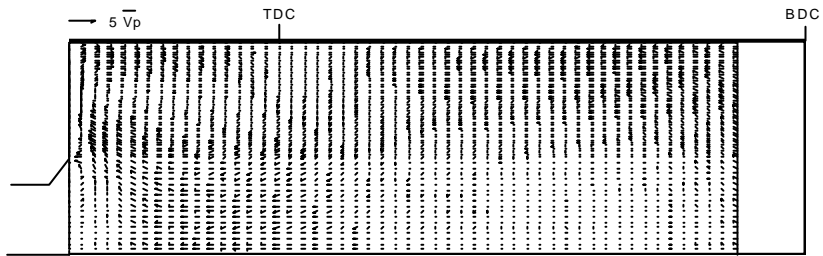


(f)

Fig.4.6 Velocity fields of modified $k - e$ model and $k - e - t$ model
 (e) modified $k - e$ model, $q=180^\circ$ (f) $k - e - t$ model, $q=180^\circ$

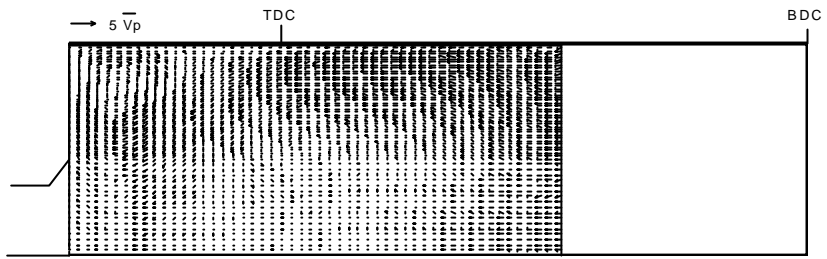


(g)

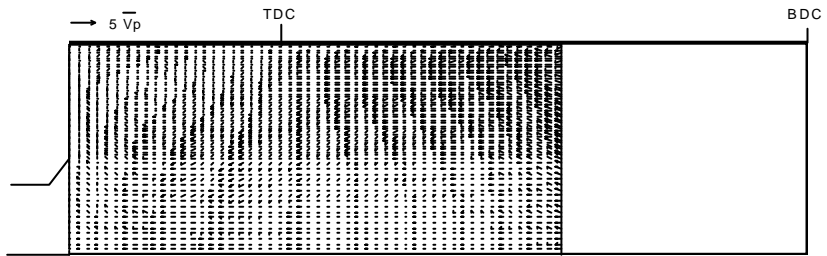


(h)

Fig.4.6 Velocity fields of modified $k - e$ model and $k - e - t$ model
 (g) modified $k - e$ model, $q=225^\circ$ (h) $k - e - t$ model, $q=225^\circ$

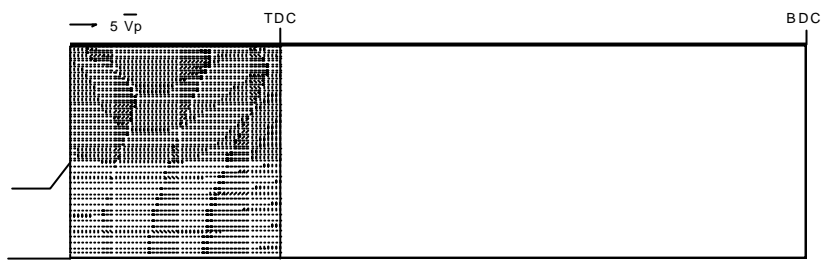


(i)

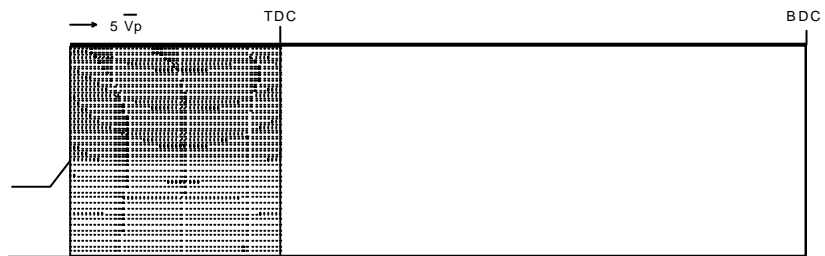


(j)

Fig.4.6 Velocity fields of modified $k - e$ model and $k - e - t$ model
 (i) modified $k - e$ model, $q=270^\circ$ (j) $k - e - t$ model, $q=270^\circ$

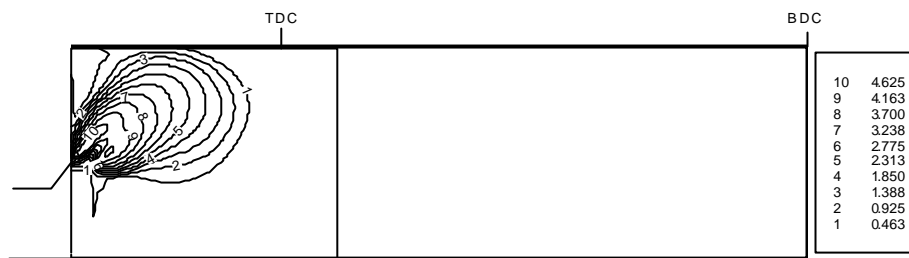


(k)

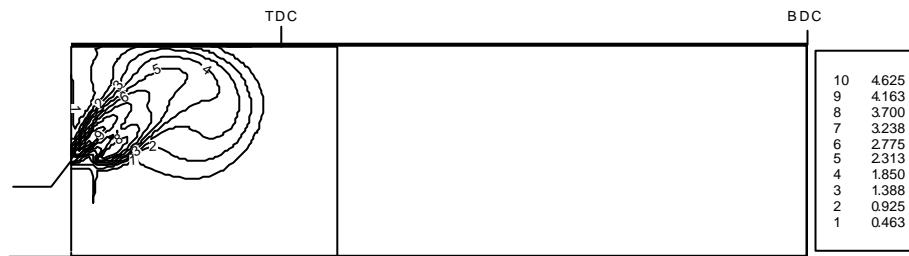


(l)

Fig.4.6 Velocity fields of modified $k - e$ model and $k - e - t$ model
 (k) modified $k - e$ model, $q=360^\circ$ (l) $k - e - t$ model, $q=360^\circ$

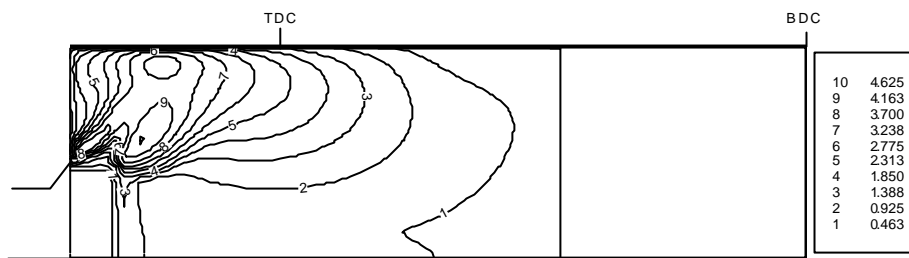


(a)



(b)

Fig.4.7 Turbulence intensities of modified $k - e$ model and $k - e - t$ model
 (a) modified $k - e$ model, $q=36^\circ$ (b) $k - e - t$ model, $q=36^\circ$



(c)

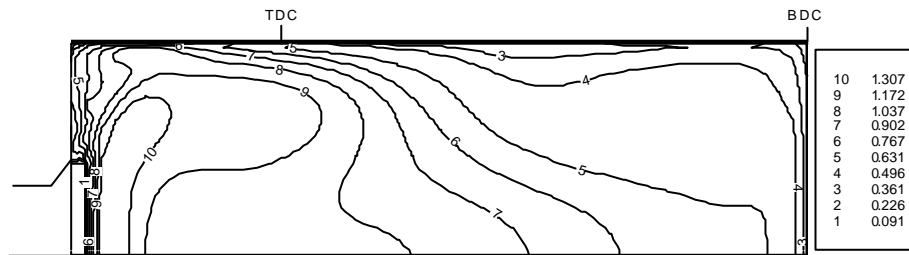


(d)

Fig.4.7 Turbulence intensities of modified $k - e$ model and $k - e - t$ model
 (c) modified $k - e$ model, $q=90^\circ$ (d) $k - e - t$ model, $q=90^\circ$

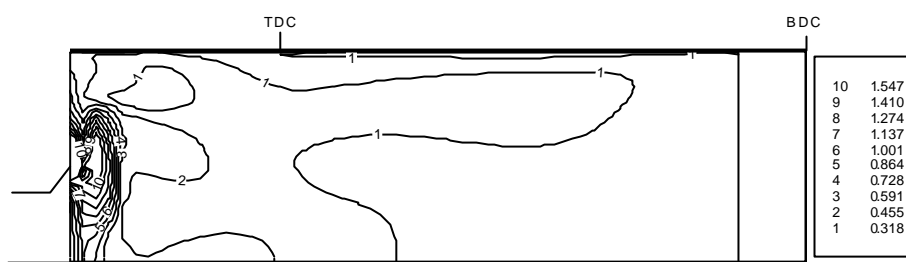


(e)



(f)

Fig.4.7 Turbulence intensities of modified $k - e$ model and $k - e - t$ model
 (e) modified $k - e$ model, $q=180^\circ$ (f) $k - e - t$ model, $q=180^\circ$

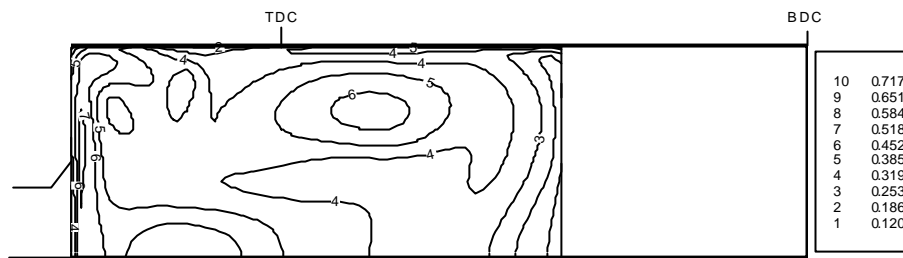


(g)



(h)

Fig.4.7 Turbulence intensities of modified $k - e$ model and $k - e - t$ model
 (g) modified $k - e$ model, $q=225^\circ$ (h) $k - e - t$ model, $q=225^\circ$

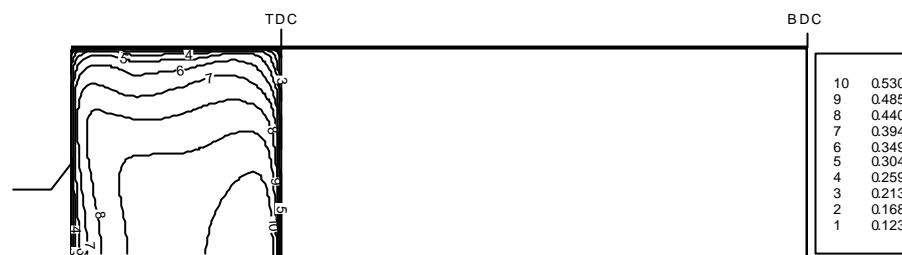


(i)

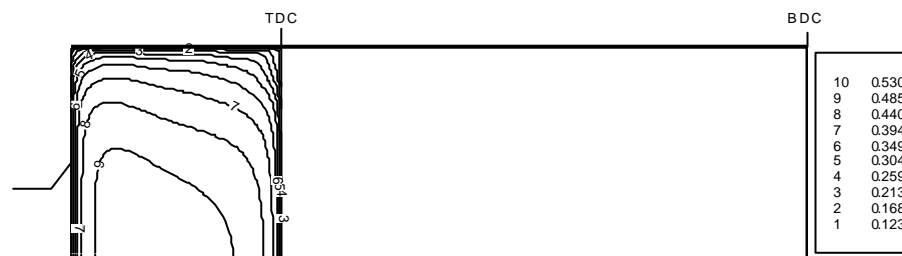


(j)

Fig.4.7 Turbulence intensities of modified $k - e$ model and $k - e - t$ model
 (i) modified $k - e$ model, $q=270^\circ$ (j) $k - e - t$ model, $q=270^\circ$



(k)



(l)

Fig.4.7 Turbulence intensities of modified $k - e$ model and $k - e - t$ model
 (k) modified $k - e$ model, $q=360^\circ$ (l) $k - e - t$ model, $q=360^\circ$

4.6

(swirl number) 0.0, 0.6, 1.2, 2.4

$k - e - t$

[65],

3

Arcoumanis et al. 4.1

1.2

. Arcoumanis

et al.

1.2

Fig.4.8

vane

3 (A3.3)

Fig.4.9

(swirl number) 1.2

, Arcoumanis et al.^[47]

$k - e - t$

, 가

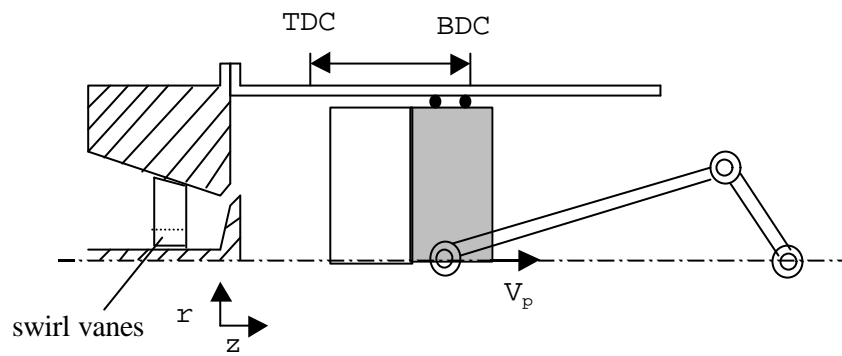


Fig.4.8 Diagram of piston-cylinder assembly with swirl vanes

Fig.4.9 (a)

90°

15mm, 40mm

. 15mm

(Fig.4.3 (a))

40mm

15mm

, 15mm

가

Fig.4.11 (e)

Fig.4.9 (b)

90°

가

15mm

. 40mm

가

Fig.4.9 (c)

(d)

270°

Fig.4.10 0.0, 1.2, 2.4

. Fig.4.11 Fig.4.12 0.6, 1.2, 2.4

, Fig.4.6 Fig.4.7

,

, 가

,

가

가 가

가

1.2

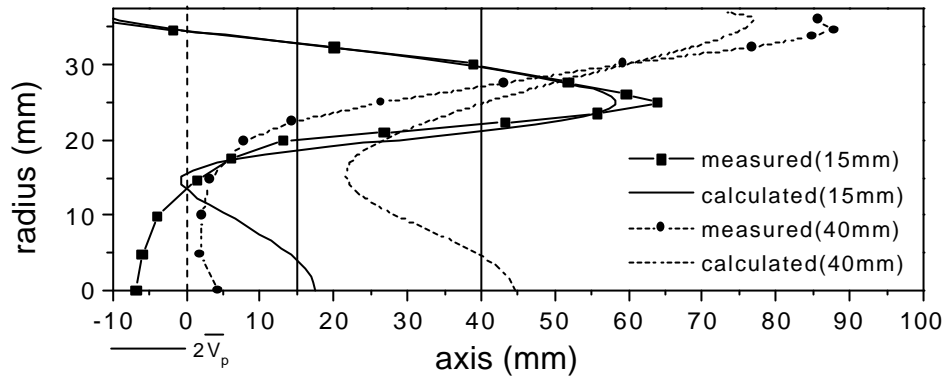
가

가 가

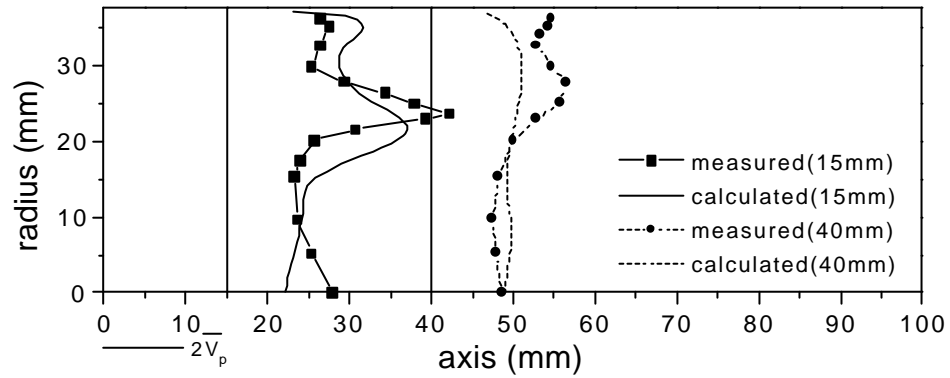
,

가가

가



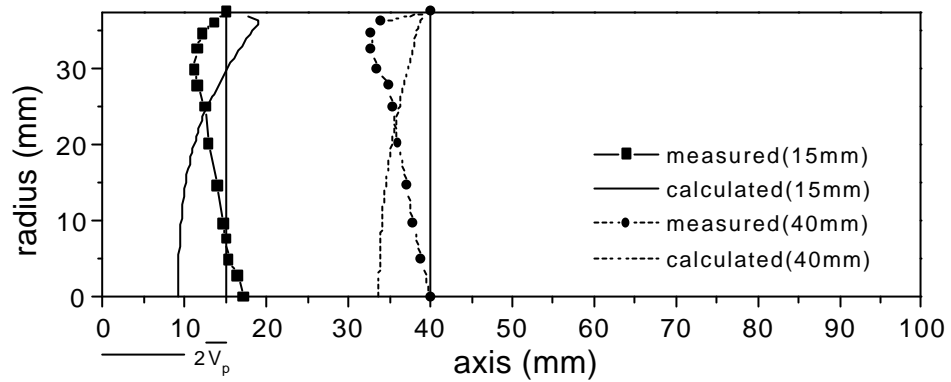
(a)



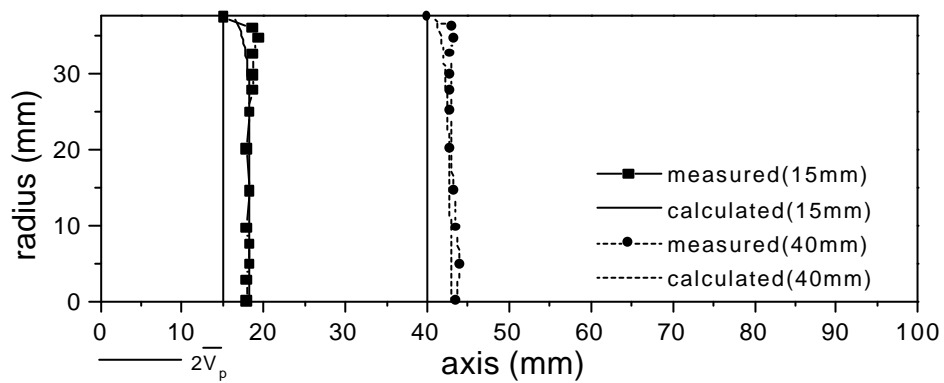
(b)

Fig.4.9 Radial profiles of axial mean velocity and rms velocity for SN=1.2 at $z=15\text{mm}, 40\text{mm}$

(a) mean velocity at $\mathbf{q}=90^\circ$ (b) rms velocity at $\mathbf{q}=90^\circ$



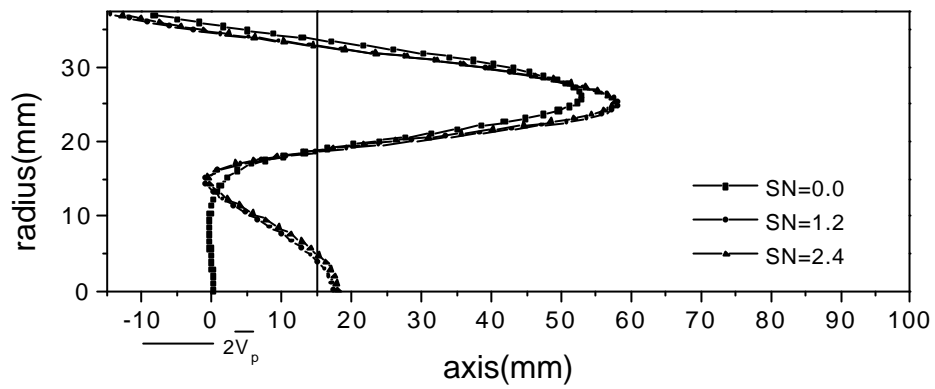
(c)



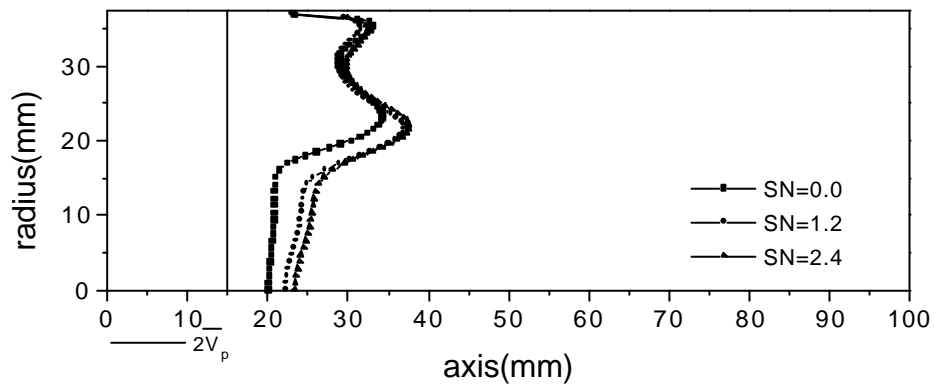
(d)

Fig.4.9 Radial profiles of axial mean velocity and rms velocity for SN=1.2 at
z=15mm, 40mm

(c) mean velocity at $q=270^\circ$ (d) rms velocity at $q=270^\circ$



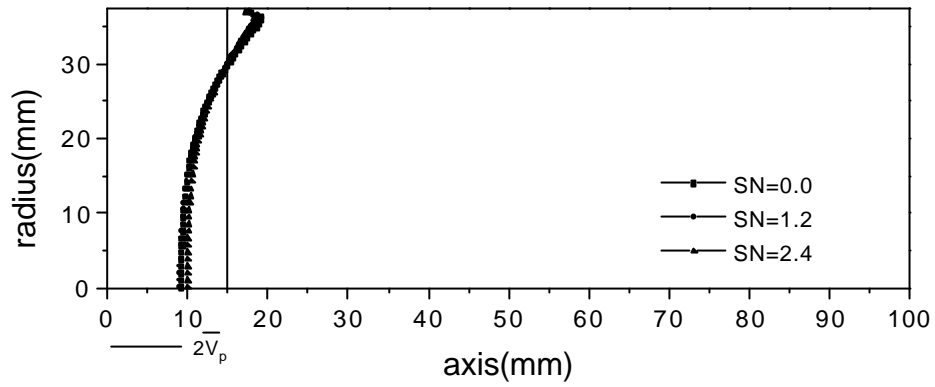
(a)



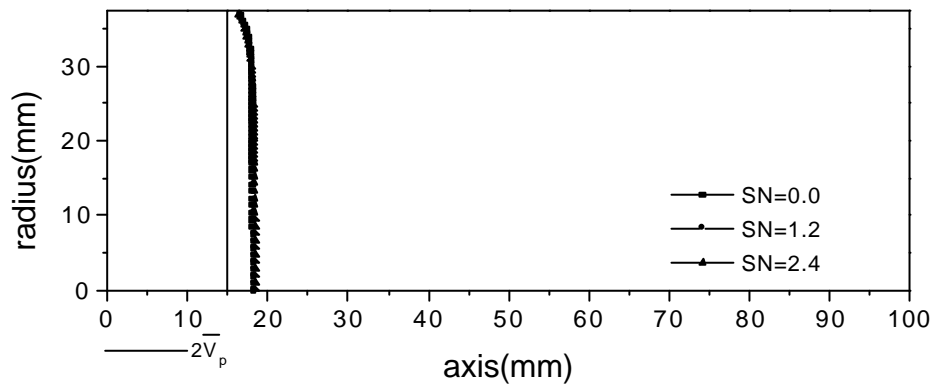
(b)

Fig.4.10 Effects of swirl on axial velocity and rms velocity for SN=0.0, 1.2, 2.4 at z=15mm

(a) mean velocity at $\mathbf{q}=90^\circ$ (b) rms velocity at $\mathbf{q}=90^\circ$



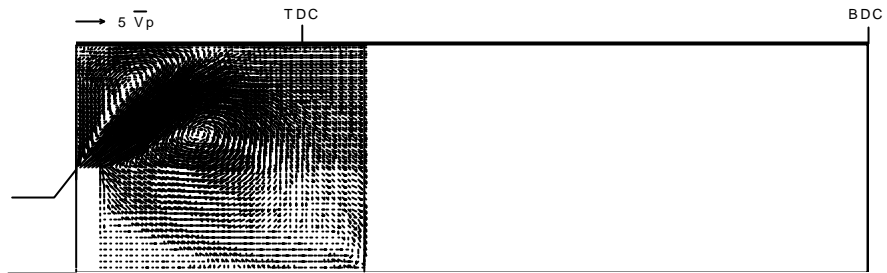
(c)



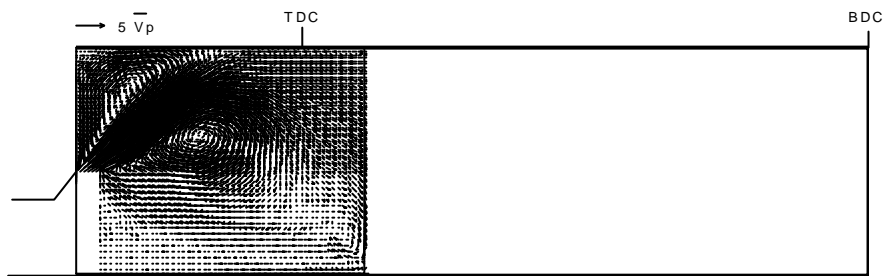
(d)

Fig.4.10 Effects of swirl on axial velocity and rms velocity for SN=0.0, 1.2, 2.4 at $z=15\text{mm}$

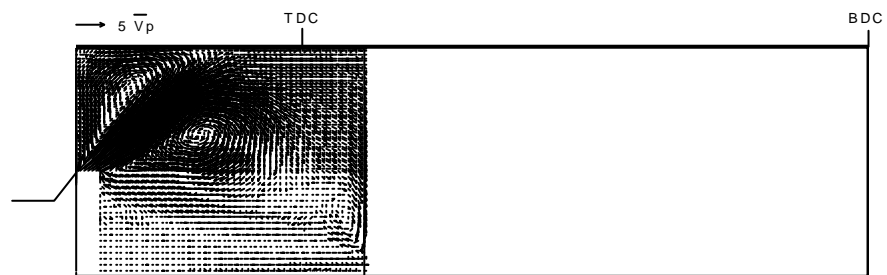
(c) mean velocity at $\mathbf{q}=270^\circ$ (d) rms velocity at $\mathbf{q}=270^\circ$



(a)

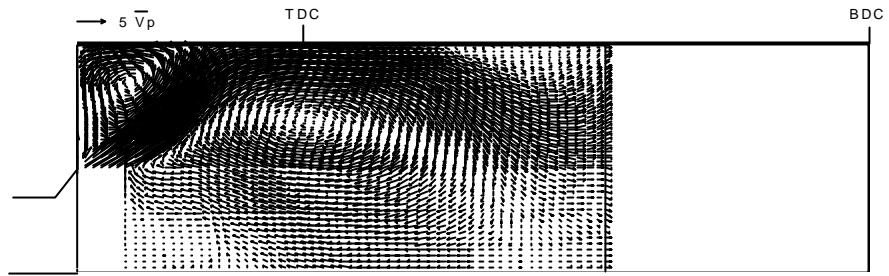


(b)

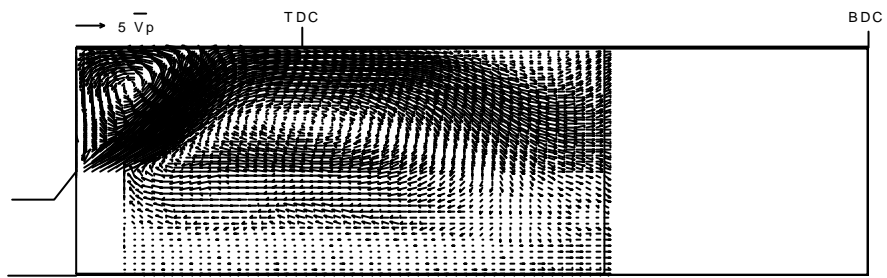


(c)

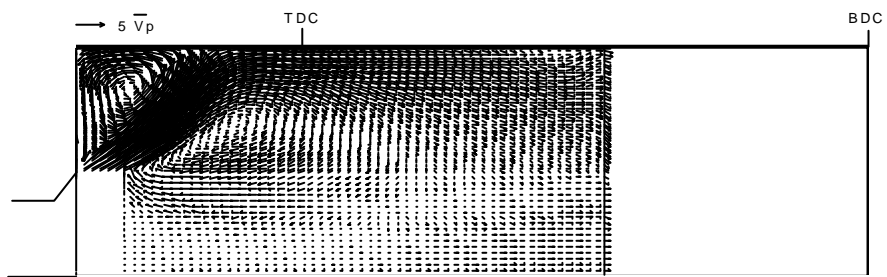
Fig.4.11 Effects of swirl on velocity fields at various crank angles
 (a) $SN=0.6, q=36^\circ$ (b) $SN=1.2, q=36^\circ$ (c) $SN=2.4, q=36^\circ$



(d)

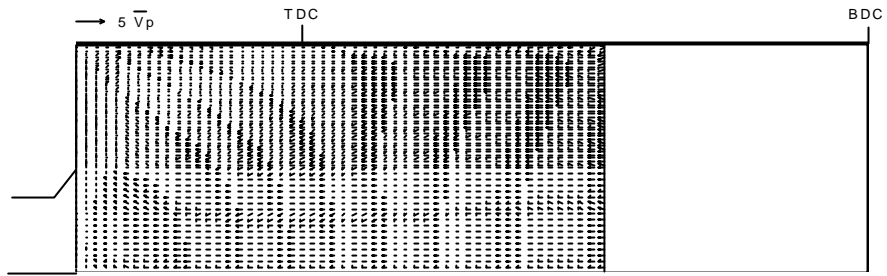


(e)

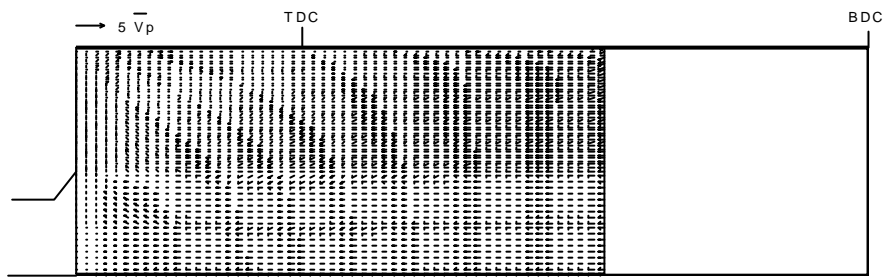


(f)

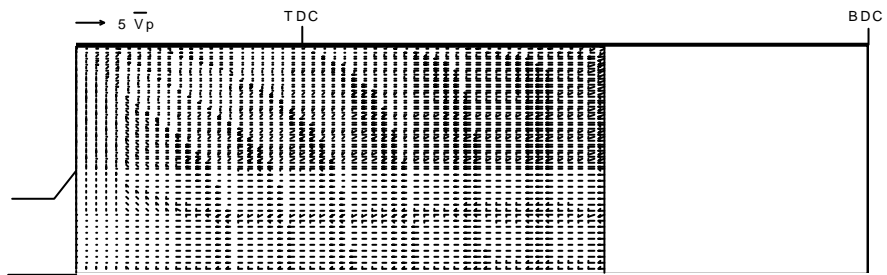
Fig.4.11 Effects of swirl on velocity fields at various crank angles
 (d) $SN=0.6, \mathbf{q}=90^\circ$ (e) $SN=1.2, \mathbf{q}=90^\circ$ (f) $SN=2.4, \mathbf{q}=90^\circ$



(g)



(h)

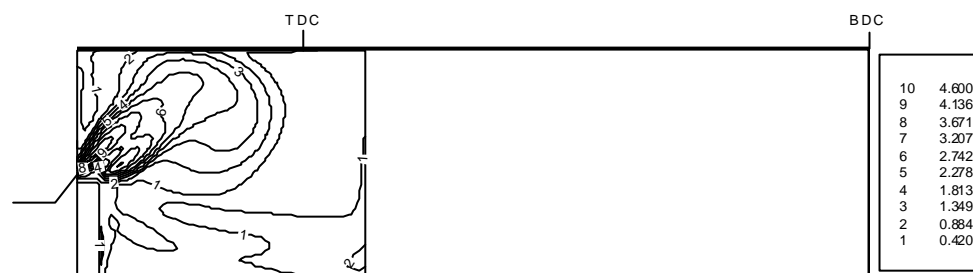


(i)

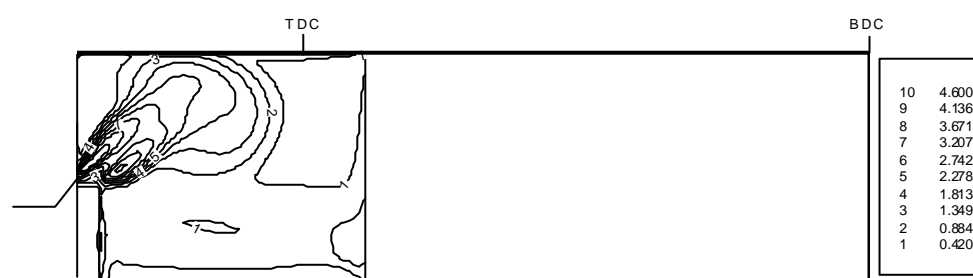
Fig.4.11 Effects of swirl on velocity fields at various crank angles
 (g) $SN=0.6, q=270^\circ$ (h) $SN=1.2, q=270^\circ$ (i) $SN=2.4, q=270^\circ$



(a)



(b)



(c)

Fig.4.12 Effects of swirl on turbulence intensity fields at various crank angles

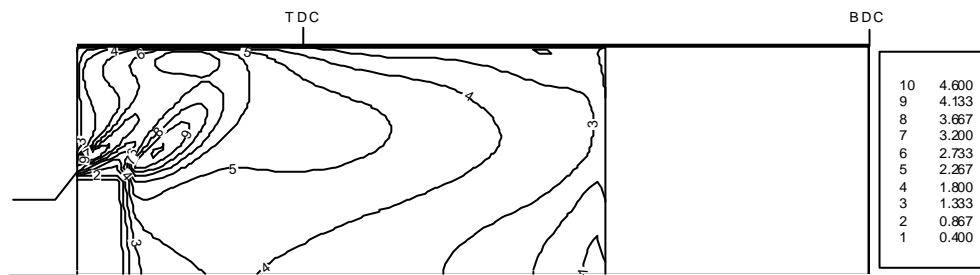
(a) SN=0.6, $q=36^\circ$ (b) SN=1.2, $q=36^\circ$ (c) SN=2.4, $q=36^\circ$



(d)



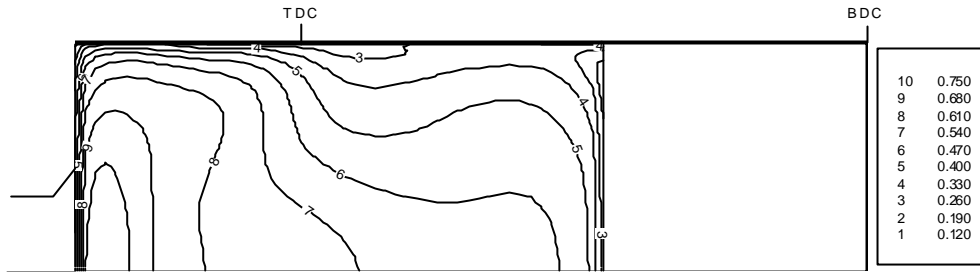
(e)



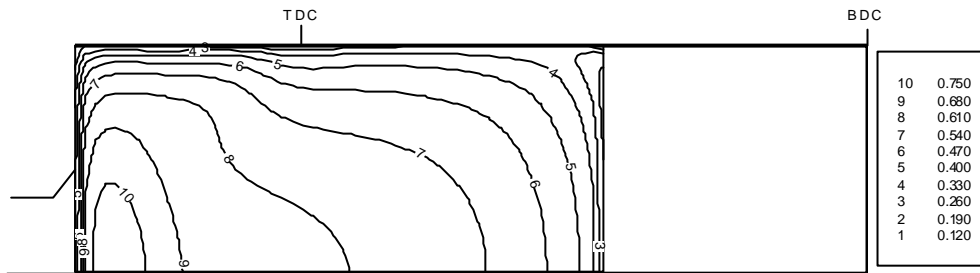
(f)

Fig.4.12 Effects of swirl on turbulence intensity fields at various crank angles

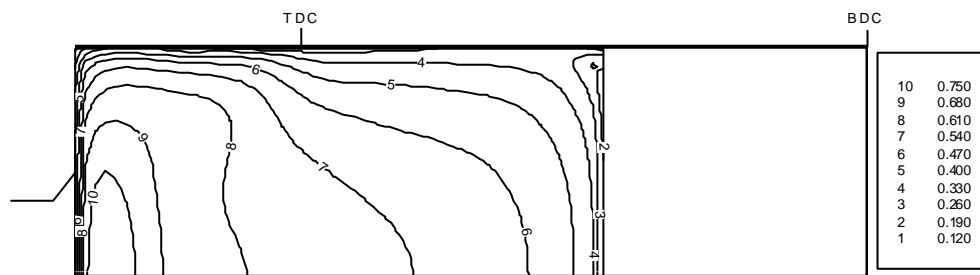
(d) SN=0.6, $q=90^\circ$ (e) SN=1.2, $q=90^\circ$ (f) SN=2.4, $q=90^\circ$



(g)



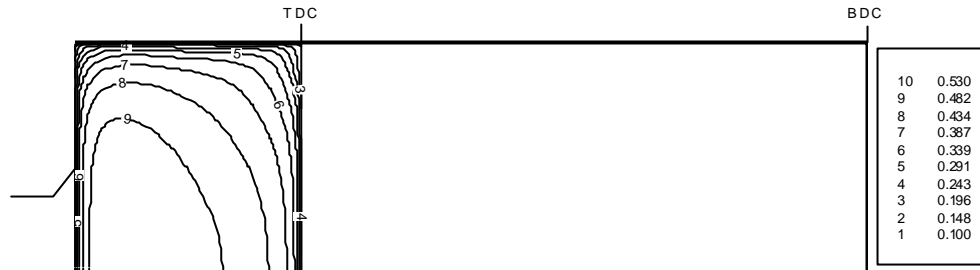
(h)



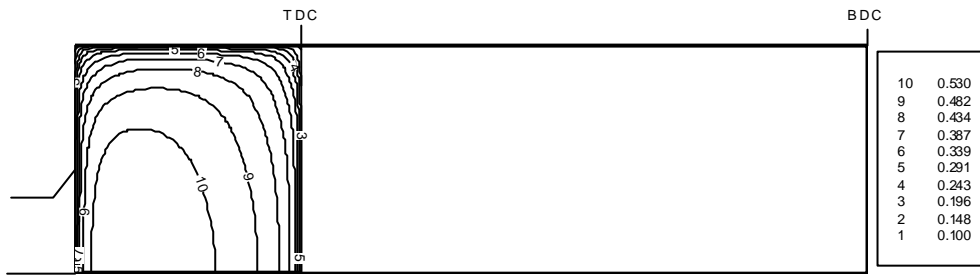
(i)

Fig.4.12 Effects of swirl on turbulence intensity fields at various crank angles

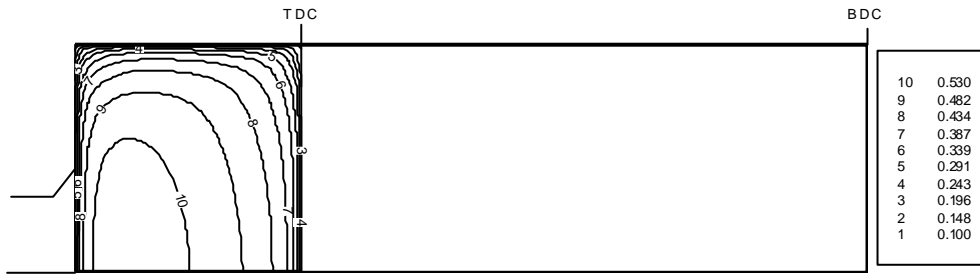
(g) $SN=0.6, q=270^\circ$ (h) $SN=1.2, q=270^\circ$ (i) $SN=2.4, q=270^\circ$



(j)



(k)



(l)

Fig.4.12 Effects of swirl on turbulence intensity fields at various crank angles

(j) SN=0.6, $q=360^\circ$

(k) SN=1.2, $q=360^\circ$

(l) SN=2.4, $q=360^\circ$

4.7

60°, 45°, 30°

Fig.4.13

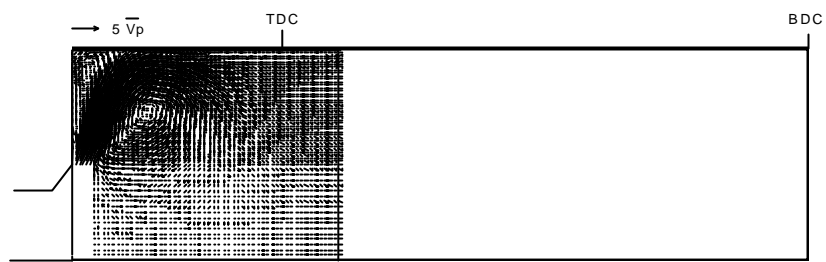
45°

가

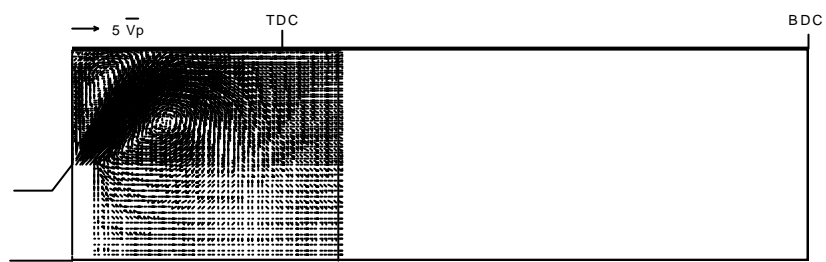
30°

가

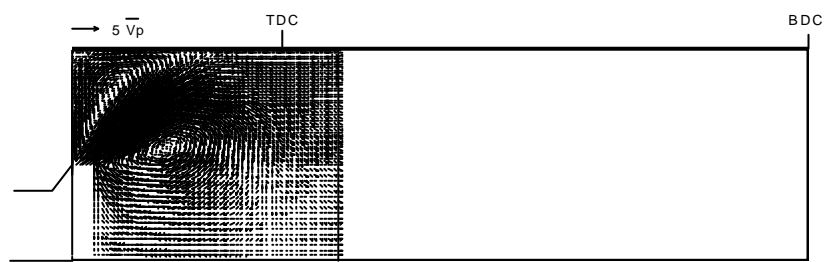
Arcoumanis et al.^[66]



(a)



(b)



(c)

Fig.4.13 Velocity fields for different valve seat angles at crank angle 36°
 (a) valve seat angle 30° (b) valve seat angle 45° (c) valve seat angle 60°

5.

, , 가

$k - e - t$

가

1) $k - e - t$

15mm

Ahmadi-Befrui et al.

$k - e$

$k - e - t$

가 $k - e$

15mm,

25mm

$k - e - t$

가 $k - e$

가

1. Richard Stone, Introduction to Internal Combustion Engines, Macmillan, pp.180-199, 1992
2. Arcoumanis, C., Whitelaw, J. H., Hentschel, W. and Schindler, K. P., "Flow and Combustion in a Transparent 1.9 Litre Direct Injection Diesel Engine", IMechE, D03293, pp.191-205, 1994
3. Stroll, H., Durst, F., Peric, M., Pereira, J. C. F. and Scheuerer, G., "Study of Laminar, Unsteady Piston-Cylinder Flows", ASME Journal of Fluids Engineering, Vol.115, pp.687-693, 1993.12
4. Morse, A. P., Whitelaw, J. H. and Yianneskis, M., "Turbulent Flow Measurements by Laser-Doppler Anemometry in Motored Piston-Cylinder Assemblies", ASME Journal of Fluids Engineering, Vol.101, pp.208-216, 1979.6
5. Choi, W. C., "Effects of Operating Speed on 3-D Mean Flows Measured at the End of Intake Stroke in an IC Engine", JSME International Journal, Vol.41, No.2, pp.338-343, 1998
6. Rouland, E., Trinite, M., Dionnet, F., Floch, A. and Ahmed, A., "Particle Image Velocimetry Measurements in a High Tumble Engine for In-Cylinder Flow Structure Analysis", SAE 972831, 1997
7. Dimopoulos, P. and Boulouchos, K., "Turbulent Flow Field Characteristics in a Motored Reciprocating Engine", SAE 972833, 1997
8. Kong, S. C. and Hong, C. W., "Multidimensional Intake Flow Modeling of a Four-Stroke Engine with Comparisons to Flow Velocity Measurements", SAE 970883, 1997
9. Ramos, J. I., Internal Combustion Engine Modeling, Hemisphere Publishing Corporation, pp.66-84, 1989
10. Heywood, J. B., "Fluid Motion Within the Cylinder of Internal Combustion Engines", ASME Journal of Fluids Engineering, Vol.109, pp.3-35, 1987.3
11. Watkins, A. P., "Flow and Heat Transfer in Piston/Cylinder Assemblies", PhD

Thesis, University of London, pp.25-37, pp.54-66, 1977

12. Witze, P. O., "A Critical Comparison of Hot-Wire Anemometry and Laser Doppler Velocimetry for I. C. Engine Applications", SAE 800132, pp.711-739, 1980

13. Gosman, A. D. and Johns, R. J. R., "Development of a Predictive Tool for In-Cylinder Gas Motion in Engines", SAE 780315, 1978

14. Ahmadi-Befrui, B., Arcoumanis, C., Bicen, A. F., Gosman, A. D., Jahanbaksh, A. and Whitelaw, J. H., "Calculation and Measurements of the flow in a Motored Model Engine and Implications for Open-Chamber, Direct-Injection Engines", NTIS DE82019033, 1982

15. Gosman, A. D., Tsui, Y. Y., and Watkins, A. P., "Calculation of Three-Dimensional Air Motion in Model Engines", FS/83/29, 1980

16. Grasso, F. and Bracco, F. V., "Computed and Measured Turbulence in Axisymmetric Reciprocating Engines", AIAA Journal, Vol.21, No.4, pp.601-607, 1983

17. Brandstatter, W., Johns, R. J. R. and Wigley, "The Effect of Inlet Port Geometry on In-Cylinder Flow Structure", SAE 850499, 1985

18. Yamada Toshio, Inoue Tokuta, Yoshimatsu Akio, Hiramatsu Takeshi and Konishi Masaaki, "In-Cylinder Gas Motion of Multivalve Engine - Three Dimensional Numerical Simulation", SAE Paper 860465, 1986

19. Priti Shah, "Mathematical Modelling of Flow and Combustion in Internal Combustion Engines", PhD Thesis, Thames Polytechnic, pp.19-43, pp.67-102, 1989

20. Monaghan, M. O. and Pettifer, H. F., "Air Motion and its Effects on Diesel Performance and Emissions", SAE 810255, 1981

21. Mao, Y., Buffat, M. and Jeandel, D., "Simulation of the Turbulent Flow Inside the Combustion Chamber of a Reciprocating Engine with a Finite Element Method", ASME Journal of Fluids Engineering, Vol.116, pp.363-369, 1994.6

22. Bahram Khalighi, "Multidimensional In-cylinder Flow Calculations and Flow Visualization in a Motored Engine", ASME Journal of Fluids Engineering, Vol.117, pp.282-288, 1995.6

23. Kong, S. C. and Hong, C. W., "Multidimensional Intake Flow Modeling of a Four-Stroke Engine with Comparisons to Flow Velocity Measurements", SAE 970883, 1997
24. Gosman, A. D., "Multidimensional Modeling of Cold Flows and Turbulence in Reciprocating Engines", SAE 850344, 1985
25. Amsden, A. A., Ramshaw, J. D., O'Rourke, P. J. and Dukowicz, J. K., "KIVA : A Computer Program for Two- and Three- Dimensional Fluid Flow with Chemical Reactions and Fuel Spray", Los Alamos National Laboratory Report LA-10245-MS, 1985
26. Launder, B. E. and Spalding, D. B., Lectures on Mathematical Models of Turbulence, Academic Press, New York, pp.90-110, 1972
27. Reynolds, W. C., "Modelling of Fluid Motions in Engines - An Introductory Overview", Combustion Modelling in Reciprocating Engines, edited by Mattavi, J. N. and Amann, C. A., Plenum Press, pp.41-65, 1980
28. Morel, T. and Mansour, N. N., "Modelling of Turbulence in Internal Combustion Engines", SAE 820040, 1982
29. El Tahry, S. H., " $k - \epsilon$ Equation for Compressible Reciprocating Engine Flows", AIAA Journal of Energy, Vol.7, No.4, pp.345-553, 1983
30. Gosman, A. D., Johns, R. J. R. and Watkins, A. P., "Development of Prediction Methods for In-Cylinder Processes in Reciprocating Engines", Combustion Modelling in Reciprocating Engines, edited by Mattavi, J. N. and Amann, C. A., Plenum Press, pp.41-65, 1980
31. Ramos, J. I., Humphrey, J. A. C. and Sirignano, W. A., "Numerical Prediction of Axisymmetric Laminar and Turbulent Flows in Motored, Reciprocating Internal Combustion Engines", SAE 790356, 1979
32. Grasso, F., Wey, M. J., Bracco, F. V. and Abraham, J., "Three Dimensional Computations of Flows in a Stratified-Charge Rotary Engine", SAE 870409, 1987
33. Ahmadi-Befrui, B., Gosman, A. D., Lockwood, F. C. and Watkins, A. P., "Multidimensional Calculation of Combustion in an Idealised Homogeneous Charge

Engine", SAE 810151, 1981

34. El Tahry, S. H., "A Numerical Study on the Effects of Fluid Motion at Inlet-valve Closure on Subsequent Fluid Motion in a Motored Engine", SAE 820035, 1982

35. El Tahry, S. H., "Application of a Reynolds Stress Model to Engine Flow Calculations", Proceedings of Symposium on Flows in Internal Combustion Engines - II, ASME-FED-20, 1984

36. Launder, B. E., Reece, G. J., and Rodi, W., "Progress in the Development of a Reynolds-Stress Turbulence Closure", J. Fluid Mech. Vol. 68, pp.537, 1975

37. Wu, C. T., Ferziger J. H. and Chapman, D. R., "Simulation and Modelling of Homogeneous Compressed Turbulence", Technical Report TF-21, Department of Mechanical Engineering, Stanford University, pp.1-80, pp.89-150, 1985.5

38. Shah, P. and Markatos, N. C., "Computer Simulation of Turbulence in Internal Combustion Engine", Int. J. Numerical Methods in Fluids, Vol.7, pp.927-953, 1987

39. Ilegbusi, J. O. and Spalding, D. B., "An Improved Version of the $k - \epsilon$ Model of Turbulence", ASME Journal of Heat Transfer, Vol.107, No.1, pp.63-69, 1985

40. Naser, J. A. and Gosman, A. D., "Flow Prediction in an Axisymmetric Inlet Valve/Port Assembly Using Variants of $k - \epsilon$ ", IMechE, D04293, pp.57-69, 1995

41. Watkins, A. P., Bo, T. and Lea, C. J., "Turbulent Flow Simulations in Model Reciprocating Engines with a Differential Stress Model", IMechE, C499/005, pp.281-290, 1996

42. Yakhot, V. and Smith, L. M., "The Renormalization Group, the ϵ -Expansion and Derivation of Turbulence Model", Journal of Scientific Computing, Vol.7, No.1, pp.35-61, 1992

43. , , , "RNG $k - \epsilon$ ",
(B), 21 , 9 , pp.1149-1164, 1997

44. , , "RNG $k - \epsilon$ /
", , 22 , 4 , pp.436-444, 1998

45. , , "

- " , 1997 , pp.103-109, 1997
46. , " , " , pp.132-139, 1999
47. Arcoumanis, C., Bicen, A. F., and Whitelaw, J. H., "Measurements in a Motored Four-stroke Reciprocating Model Engine", ASME Journal of Fluids Engineering, Vol.104, pp.235~241, 1982
48. Ahmadi-Befrui, B., Gosman, A. D., Jahanbakhsh, A. and Watkins, A.P., "The DICE Computer Codes for Prediction of Laminar and Turbulent Flow and Heat Transfer in Idealised Motored Diesel Engine Combustion Chambers", Imperial College of Science and Technology, pp.8-22, 1990. 11
49. , _____, , pp.264~289, 1994
50. Nagano, Y. and Tagawa, M., "An Improved $k - \epsilon$ Model for Boundary Layer Flows", ASME Journal of Fluids Engineering, Vol.112, pp.33-39, 1990.3
51. Hanjalic, K. and Launder, B. E., "A Reynolds Stress Model of Turbulence and its Application to Thin Shear Flows", J. Fluid Mech., Vol.52, pp.609-638, 1972
52. Lebrere, L., Buffat, M., Penven, L. L. and Dillies, B., "Application of Reynolds Stress Modeling to Engine Flow Calculations", ASME Journal of Fluids Engineering, Vol.118, pp.710-721, 1996.12
53. Kido, H., Nakashima, K., Tajima, H. and Kitagawa, T., " A Modified $k - \epsilon$ Turbulence Model for In-Cylinder Gas Flow", Proc. of Int. Sym. on Diagnostics and Modeling of Combustion in Reciprocating Engines, pp.221-226, 1985
54. Versteeg, H. K. and Malalasekera, W., An Introduction to Computational Fluid Dynamics, The Finite Volume Method, Longman Scientific & Technical, pp.135-155, 1995
55. Patankar S. V., Numerical Heat Transfer and Fluid Flow, Hermisphere Publishing Corporation, pp.126-131, 1980
56. Issa, R. I., "Solution of the Implicitly Discretised Fluid Flow Equations by Operator-Splitting", Journal of Computational Physics 62, pp.40~65, 1985

57. Issa, R. I., Gosman, A. D. and Watkins, A. P., "The Computation of Compressible and Incompressible Recirculating Flows by a Non-iterative Implicit Scheme", *Journal of Computational Physics* 62, pp.66~82, 1986
58. Blair, G. P., Lau, H. B., Cartwright, a., Raghunathan, B. D. and Mackey, D. O., "Coefficients of Discharge at the Aperature of Engines", SAE 952138, pp.71-85, 1995
59. Blair, G. P. and Drouin, F. M. M., "Relationship Between Discharge Coefficients and Accuracy of Engine Simulation", SAE 962527, pp.151-162, 1996
60. Danov, S., "Identification of Discharge Coefficients for Flow Through Valves and Ports of Internal Combustion Engines", SAE 970642, pp.279-286, 1997
61. Bicen, A. F., Vafidis, C. and Whitelaw, J. H., "Steady and Unsteady Airflow Through the Intake Valve of a Reciprocating Engine", *ASME Journal of Fluids Engineering*, Vol.107, pp.413~420, 1985.9
62. Butler, T. D., Amsden, A. A., O'Rourke, P. J. and Ramshaw, J. D., "KIVA : A Comprehensive Model for 2D and 3D Engine Simulation", SAE 850554, 1985
63. , , "
", , 11 , 3 , pp.395-408, 1987
64. Hoult, D. P. and Wong, V. W. "The Generation of Turbulence in an Internal Combustion Engine", Combustion Modeling in Reciprocating Engines, edited by Mattavi, J. N. and Amann, C. A., pp.131~160, Plenum Press, New York, 1980
65. , "
", , , pp.143-144, 1990
66. Gosman, A. D., "Flow Processes in Cylinders", The Thermodynamics and Gas Dynamics of Internal Combustion Engines, Volume II, edited by Horlock, J. H. and Winterbone, D. E., pp.616-772, 1986

1.

Fig.A1.1 (multi-layered structure)

(viscous sublayer), 가 (inertial sublayer),
 가 (buffer layer)

가 , , ,
 가 ,
 가 .

(wall function)

y , \mathbf{r} ,

\mathbf{m} \mathbf{t}_w ,

y^+ u^+ (law of the wall)

$$u^+ = \frac{U}{u_t} = f\left(\frac{\mathbf{m}u_t y}{\mathbf{m}}\right) = f(y^+) \quad (A1.1)$$

$u_t (= \sqrt{\mathbf{t}_w / \mathbf{r}})$ (friction velocity)

(A1.1) Fig.A1.1 ,

$$u^+ = y^+ \quad (A1.2)$$

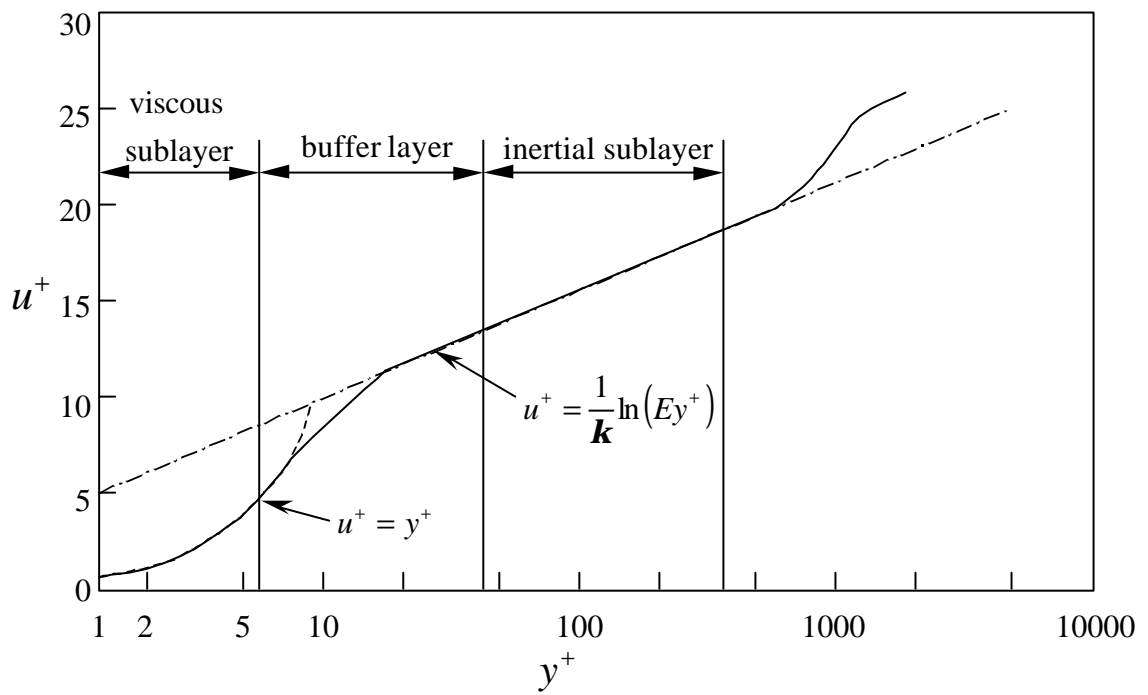


Fig.A1.1 Velocity distribution near a solid wall

$$u^+ = \frac{1}{k} \ln y^+ + B = \frac{1}{k} \ln(Ey^+) \quad (A1.3)$$

k Von Karman 0.4187, E
9.793 ($B = 5.5$)

y_p 가 (A1.3)

(budget)

가 ,

$$u^+ = \frac{1}{k} \ln(Ey_p^+) \quad (A1.4)$$

$$k = \frac{u_t^2}{\sqrt{C_m}} \quad (A1.5)$$

$$\mathbf{e} = \frac{u_t^3}{ky} \quad (A1.6)$$

no-slip ($u = v = 0$)

$$T^+ = -\frac{(T_p - T_w)C_p \mathbf{m}_t}{q_w} = \mathbf{s}_{T,t} \left[u^+ + P \left(\frac{\mathbf{s}_{T,l}}{\mathbf{s}_{T,t}} \right) \right] \quad (A1.7)$$

T_p y_p , T_w , q_w ,

C_p , $\mathbf{s}_{T,t}$ Prandtl, $\mathbf{s}_{T,l}$ Prandtl. P

'pee-function', Prandtl Prandtl

$$\begin{aligned}
P\left(\frac{\mathbf{s}_{T,l}}{\mathbf{s}_{T,t}}\right) &= 9.24 \left[\left(\frac{\mathbf{s}_{T,l}}{\mathbf{s}_{T,t}}\right)^{0.75} - 1 \right] \\
&\times \left\{ 1 + 0.28 \exp \left[-0.007 \left(\frac{\mathbf{s}_{T,l}}{\mathbf{s}_{T,t}}\right) \right] \right\}
\end{aligned}
\tag{A1.8}$$

2.

가

가 (equivalent ideal flow)

가

가

(discharge coefficient) C_D

$$C_D = \frac{\text{actual mass flow}}{\text{ideal mass flow}}$$

A_E (reference area)

A_R

$$C_D = \frac{A_E}{A_R} \quad (\text{A2.1})$$

T_0

p_0

$$T_0 = T + \frac{V^2}{2c_p} \quad (\text{A2.2})$$

$$\left(\frac{T}{T_0}\right) = \left(\frac{p}{p_0}\right)^{\frac{\gamma-1}{\gamma}} \quad (\text{A2.3})$$

$$(A2.2) \quad M = \frac{V}{a} \quad (a = \sqrt{gRT})$$

$$\frac{T_0}{T} = 1 + \frac{g-1}{2} M^2 \quad (A2.4)$$

$$\frac{p_0}{p} = \left(1 + \frac{g-1}{2} M^2 \right)^{\frac{g}{g-1}} \quad (A2.5)$$

\dot{m}

$$\dot{m} = \rho AV$$

$$p \quad T$$

$$\frac{\dot{m}_{ideal} \sqrt{gRT_0}}{Ap_0} = gM \left(1 + \frac{g-1}{2} M^2 \right)^{\frac{-(g+1)}{2(g-1)}} \quad (A2.6)$$

$$\frac{\dot{m}_{ideal} \sqrt{gRT_0}}{Ap_0} = g \left(\frac{p}{p_0} \right)^{\frac{1}{g}} \left[\frac{2}{g-1} \left\{ 1 - \left(\frac{p}{p_0} \right)^{\frac{g-1}{g}} \right\} \right]^{\frac{1}{2}} \quad (A2.7)$$

$$p_0 \quad T_0 \quad ,$$

(throat) 가

(choke)

p_T p_0 가

$$\frac{p_T}{p_0} = \left(\frac{2}{g+1} \right)^{\frac{g}{g-1}} \quad (\text{A2.8})$$

$\frac{p_T}{p_0}$ 가

$$\frac{\dot{m}_{ideal} \sqrt{gRT_0}}{A_T p_0} = g \left(\frac{2}{g+1} \right)^{\frac{(g+1)}{2(g-1)}} \quad (\text{A2.9})$$

$$g=1.4 \qquad 0.528, \quad g=1.3 \qquad 0.546$$

가

$$\dot{m} = \frac{C_D A_R p_0}{\sqrt{RT_0}} \left(\frac{p_T}{p_0} \right)^{\frac{1}{g}} \left[\frac{2g}{g-1} \left\{ 1 - \left(\frac{p_T}{p_0} \right)^{\frac{g-1}{g}} \right\} \right]^{\frac{1}{2}} \quad (\text{A2.10})$$

$$\frac{p_T}{p_0} \leq \left(\frac{2}{g+1} \right)^{\frac{g}{g-1}}$$

$$\dot{m} = \frac{C_D A_R p_0}{\sqrt{RT_0}} g^{\frac{1}{2}} \left(\frac{2}{g+1} \right)^{\frac{g+1}{2(g-1)}} \quad (\text{A2.11})$$

(poppet)

(A2.10) (A2.11)

p_0

$T_0,$

A_R (reference

area) . 가 p_0
, p_T . 가
 p_0 , p_T
 C_D . ,
 $C_D A_R$ (effective flow area) A_E .
가 ,

$$A_E = r_0 \left[2 p_0 r_0 \frac{g}{g-1} \left(\frac{p}{p_0} \right)^{\frac{2}{g}} \left\{ 1 - \left(\frac{p}{p_0} \right)^{\frac{g-1}{g}} \right\} \right]^{\frac{1}{2}} \quad (A2.12)$$

가 , $\frac{\rho D_v^2}{4}$,
 $\frac{\rho D_p^2}{4}$, , (curtain) $\rho D_v L_v$
가 , 가

$$A_C = \rho D_v L_v \quad (A2.13)$$

. Fig.A2.1

/

$$A_m = \mathbf{p} L_v \cos \mathbf{b} \left(D_v - 2w + \frac{L_v}{2} \sin 2\mathbf{b} \right) \quad (\text{A2.14})$$

$$\mathbf{b}, L_v, D_v, w$$

$$\left[\left(\frac{D_p^2 - D_s^2}{4D_m} \right) - w^2 \right]^{\frac{1}{2}} + w \tan \mathbf{b} \geq L_v > \frac{w}{\sin \mathbf{b} \cos \mathbf{b}}$$

$$A_m = \mathbf{p} D_m \left[(L_v - w \tan \mathbf{b})^2 + w^2 \right]^{\frac{1}{2}} \quad (\text{A2.15})$$

$$D_p, D_s, D_m$$

$$(D_v - w)$$

가

$$L_v \geq \left[\left(\frac{D_p^2 - D_s^2}{4D_m} \right) - w^2 \right]^{\frac{1}{2}} + w \tan \mathbf{b}$$

$$A_m = \frac{\mathbf{p}}{4} (D_p^2 - D_s^2) \quad (\text{A2.16})$$

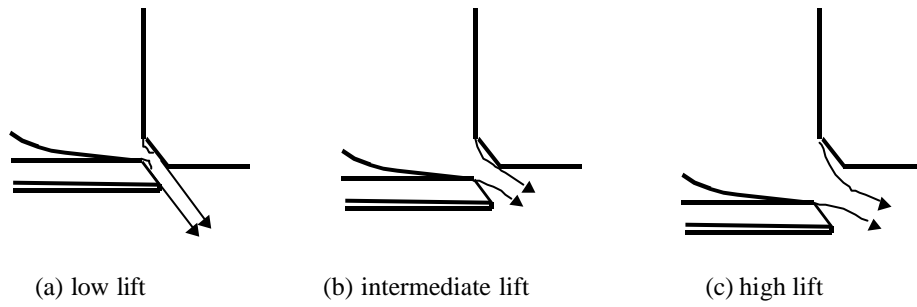
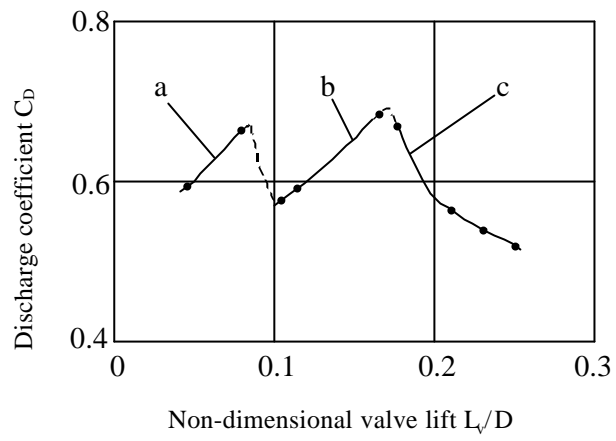


Fig.A2.1 Discharge coefficient of typical poppet valve

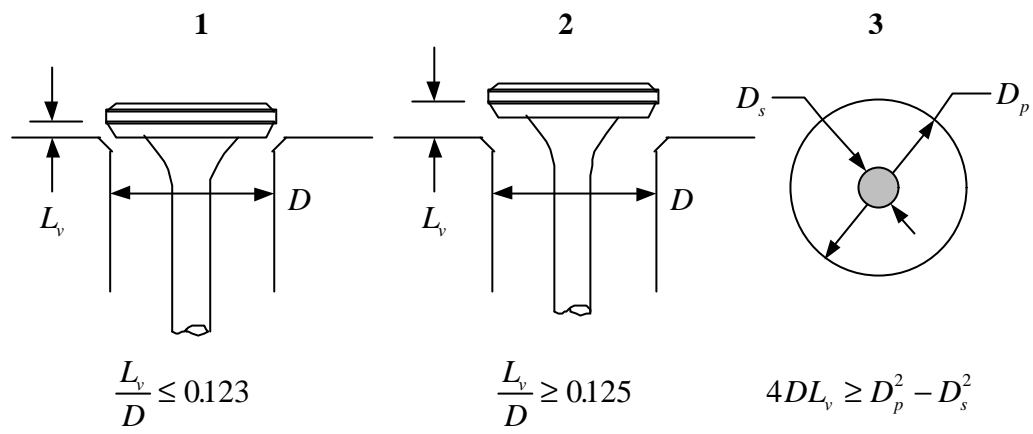


Fig.A2.2 Three stage of valve lift

3.

ratio)가 . 가 , (swirl number) (swirl

. Fig. A3.1

$$= \int_{R_1}^{R_0} \left(\mathbf{r}U_0 \cdot \frac{2\mathbf{p}dr}{\cos \mathbf{a}} \right) rW \quad (\text{A3.1})$$

$$= \int_{R_1}^{R_0} \left(\mathbf{r}U_0 \cdot \frac{2\mathbf{p}dr}{\cos \mathbf{a}} \right) V \quad (\text{A3.2})$$

SN

$$SN = \frac{\frac{\mathbf{r}U_0\mathbf{p}W}{\cos \mathbf{a}} \cdot \frac{2}{3}(R_0^3 - R_1^3)}{\frac{\mathbf{r}U_0\mathbf{p}V}{\cos \mathbf{a}} \cdot (R_0^2 - R_1^2)L} \quad (\text{A3.3})$$

$$= \frac{2}{3} \frac{W}{V} \frac{R_0}{L} \frac{\left[1 - \left(\frac{R_1}{R_0} \right)^3 \right]}{\left[1 - \left(\frac{R_1}{R_0} \right)^2 \right]}$$

W , V , R_0 , L

R_1

$$R_1 = R_0 - L \sin \mathbf{a} \cos \mathbf{a} \quad (\text{A3.4})$$

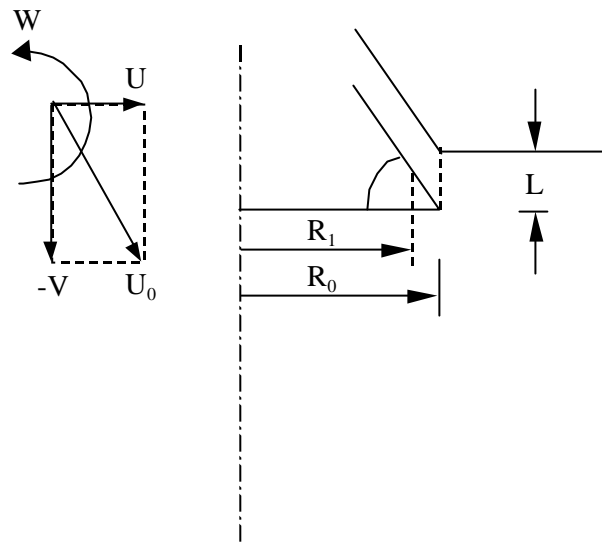


Fig.A3.1 Coordinate system around valve